Evidence for boundary layer oxygen diffusion limitation as a key driver of asteroid wasting

Citlalli A. Aquino[1*], Ryan M. Besemer[2*], Christopher M. DeRito[3], Jan Kocian[4], Ian R. Porter[5], Peter Raimondi[6], Jordan E. Rede[3], Lauren M. Schiebelhut[7], Jed P. Sparks[8], John P. Wares[9], Ian Hewson[3†]

[1]Department of Biology, Estuary and Ocean Science Center, San Francisco State University, Romberg Tiburon Campus, 3150 Paradise Dr, Tiburon CA 94132 USA

[2]Center for Marine Science, University of North Carolina Wilmington, 5600 Marvin K Moss Ln, Wilmington, NC 28409 USA

[3]Department of Microbiology, Cornell University, Wing Hall 403, Ithaca NY 14853 USA

[4]Independent Scientist, Leland WA 98376 USA

[5]Department of Clinical Sciences, College of Veterinary Medicine, Cornell University, 602 Tower Rd, Ithaca, NY 14853 USA

[6]Institute of Marine Sciences, Department of Ecology & Evolutionary Biology, University of California Santa Cruz, 1156 High Street, Santa Cruz, CA 95064 USA

[7]Life and Environmental Sciences, University of California Merced, 5200 North Lake Rd. Merced, CA 95343 USA

[8]Department of Ecology & Evolutionary Biology, Cornell University, Corson Hall, Ithaca NY 14853 USA

[9]Department of Genetics, University of Georgia, 30602 120 W Green St, Athens, GA 30602 USA

*Denotes equal author contribution

[†]Corresponding Author: Department of Microbiology, Wing Hall 403, Cornell University, Ithaca NY 14853 USA, Email: hewson@cornell.edu, Tel: +16072550151

Running Head: **Boundary Layer Microorganisms Affect Asteroid Wasting**

Author Contributions: LMS and IH designed research; CA, RMB, CMD, JK, IRP, PR, JER, LMS, JPS and IH performed research; CA, RMB, CMD, IRP, PR, JER, LMS, JPS, JPW and IH conducted review and wrote the manuscript; PR and IH provided funding for the research.

Keywords: Sea Star Wasting, Oxygen, Heterotroph, Remineralization, Phytoplankton

ABSTRACT

Sea star wasting (SSW) disease describes a condition affecting asteroids that resulted in significant Northeastern Pacific population decline following a mass mortality event in 2013. The etiology of sea star wasting is unresolved. We hypothesize that asteroid wasting is a sequela of microbial organic matter remineralization near respiratory surfaces which leads to boundary layer oxygen diffusion limitation (BLODL). Wasting lesions were induced in *Pisaster ochraceus* by enrichment with a variety of organic matter (OM) sources. Microbial assemblages inhabiting tissues and at the asteroid-water interface bore signatures of copiotroph proliferation before wasting onset, concomitant with and followed by the proliferation of putatively facultative and strictly anaerobic taxa. Bacterial cell abundance increased dramatically prior to wasting onset in experimental incubations. Wasting susceptibility was significantly correlated with rugosity (a key determinant of boundary layer thickness) of animal surfaces. At a semi-continuously monitored field site (Langley Harbor), wasting predictably occurred at annual peak or decline in phytoplankton biomass. Finally, wasting individuals from 2013 – 2014 bore stable isotopic signatures reflecting anaerobic processes and altered C and N metabolisms. These convergent lines of evidence support our hypothesis that BLODL is associated with wasting both in contemporary SSW events and during the 2013-2014 SSW mass mortality event, potentially driven by phytoplankton-derived OM. The impacts of BLODL may be more pronounced under higher temperatures due to lower O_2 solubility, in more rugose asteroid species due to restricted hydrodynamic flow, and in larger specimens due to their lower surface area to volume ratios which affects diffusive respiratory potential.

Significance Statement: Sea star wasting disease affected multiple species of asteroids and has caused mass mortality in the Northeast Pacific Ocean since 2013. The underlying cause of wasting is unknown. We hypothesized that wasting may be due to respiratory deficit resulting from heterotrophic bacterial consumption of organic matter, resulting in oxygen depletion, near animal surfaces. Here, we provide convergent lines of evidence for this hypothesis, including shifts in microbial assemblage abundance and composition during wasting which suggest surface tissues experience sub-oxic conditions. Organic matter amendment results in asteroid wasting, and we provide elemental evidence for anaerobic conditions during mass mortality in 2013-2014.

Our results are entirely consistent with environmental correlates of wasting in prior studies, including thermal stress and upwelling.

INTRODUCTION

Sea star wasting (SSW) disease describes a suite of clinical signs in asteroids including loss of turgor, arm twisting, epidermal ulceration, limb autotomy, and death. The condition gained prominence in 2013 when it caused mass mortality of >20 asteroid species in the Northeastern Pacific (Hewson et al. 2014) with continuous observations since (Jaffe et al. 2019; Miner et al. 2018). However, lesions compatible with SSW in various asteroid species have been reported since at least 1896 in the Eastern US (Mead 1898), and at many locations globally (reviewed in Hewson et al. 2019). The cause of SSW is unresolved. Early reports that SSW was associated with a densovirus (Hewson et al. 2014) were refuted by subsequent investigation that failed to show a consistent association between the virus and presence of disease (Hewson et al. 2018), and recent description of persistent infection by a related densovirus in three species of grossly normal sea stars (Jackson et al. 2020) suggest this virus to be a component of normal microbiome. Furthermore, wasting is not consistently associated with any bacterial or microbial eukaryotic organism (Hewson et al. 2018). Environmental conditions, including elevated water temperatures (Eisenlord et al. 2016; Kohl et al. 2016), lower water temperatures and higher pCO_2 (Menge et al. 2016), and meteorological conditions (Hewson et al. 2018a) correspond with wasting at distinct locations. Recent modelling studies suggest repeated sea surface temperature anomalies may correlate with wasting (Aalto et al. 2020). Reports of SSW spread between adjacent geographic locations, through public aquarium intakes, and challenge experiments with tissue homogenates suggested a transmissible etiology (Bucci et al. 2017; Hewson et al. 2014). However, there is a lack of mechanistic understanding how SSW is generated in affected individuals.

Here we provide convergent evidence that asteroid wasting is a consequence of boundary layer oxygen diffusion limitation (BLODL). First, microbiome changes during wasting progression suggest that heterotrophic (copiotrophic) microorganisms proliferate before wasting, followed by growth of taxa with facultative or strictly anaerobic metabolism, indicating depletion of dissolved O_2 near animal surfaces and within tissues. We demonstrate that wasting can result

from suboxic water column conditions, and that wasting lesions are induced by amendment with organic matter. Next, we illustrate that wasting susceptibility is related to between-species variation in rugosity (and subsequent impacts on boundary layer height), which ultimately relates to gas flux potential. Finally, we demonstrate that wasting asteroids from the 2013-2014 mass mortality event bore stable isotopic signatures that reflect anaerobic microbial processes and altered C and N metabolisms compared to their asymptomatic sympatric counterparts.

MATERIALS AND METHODS:

For detailed experimental protocols and statistical analyses performed please refer to the *Supplemental Information*. Study of microbiome shifts during wasting progression in the absence of external stimuli directed an experiment to examine the impact of suboxic conditions on SSW genesis. Hypotheses generated from these observations directed study of organic matter (OM) impacts on SSW. Following this, we examined asteroid rugosity as it relates to SSW susceptibility, and sought evidence linking biological oceanographic conditions to wasting through time series analysis at a field site. Finally, we examined stable isotopic signatures of anaerobic processes in samples collected from 2013-2014 to examine evidence for anaerobic conditions during mass mortality.

Wasting progression in the absence of external stimuli: We examined longitudinal changes in *Pisaster ochraceus* microbiome composition during wasting progression in two studies to understand potentially pathogenic taxa. In both experiments, *P. ochraceus* were collected from sites near Santa Cruz, CA, in Summer 2018, and experiments performed at the Long Marine Laboratory at UC Santa Cruz in flow-through sea tables. In the first experiment, we focused on microbial community changes in lesion margin tissues, while in the second experiment, we also examined microbial community changes in artificial scar abrasions to parse microbial taxa unique to SSW-affected tissues. In addition to animal mass and gross appearance, temperature, salinity and dissolved oxygen (DO) were measured using both HOBO loggers (Onset) or a handheld probe (YSI-3000).

Impact of suboxic conditions on wasting in Asterias forbesi: We examined the impacts of reduced oxygen conditions on *Asterias forbesi* wasting in the context of microbiome

composition. Asteroid specimens (n = 24 specimens) were transported to the Department of Microbiology at Cornell University. There, asteroids were divided into two recirculating aquarium systems. One system was continuously sparged with N_2, resulting in a ~39% decrease in DO, while the second maintained saturated DO conditions throughout the experiment. Specimens were monitored daily for SSW lesions. Samples for microbial community analyses were collected by body wall biopsy punch (i.e. surface and tissue bound microorganisms) and by surface swab (i.e. surface bound microorganisms).

Impact of OM enrichment on sea star wasting: We examined the impact of variable-source OM enrichment on asteroid wasting to test whether enrichment caused bacterial abundance and microbial composition shifts consistent with the boundary layer oxygen diffusion limitation (BLODL) hypothesis. *Pisaster ochraceus* (n = 20 specimens) were obtained from the jetty at Bodega Bay in Summer 2019, and experiments were performed in flow-through large volume sea tables at the Bodega Bay Marine Laboratory. Asteroids were subject to daily doses of 4 organic matter sources: particulate OM (POM; > 10 µm) of a dense *Dunaliela tertiolecta* culture; POM (>10 µm) concentrated from aquarium inflow water; and Peptone. Bacterial abundance in aquarium water and in samples retrieved from specimen surfaces was examined by SYBR Gold epifluorescence microscopy (Noble and Fuhrman 1998; Porter and Feig 1980; Shibata et al. 2006). Samples of lesion margin tissue, body wall and surface swabs were collected consistently with suboxic experiments detailed earlier.

Additional experimental challenges of* Pisaster ochraceus*: Additional experiments to determine the impacts of desiccation, aquarium water replenishment rate (i.e. flow rate), and challenge with wasted asteroid tissue homogenates were performed in Summer 2018 at the Long Marine Laboratory at UC Santa Cruz. Experiments were performed in flow-through sea tables receiving influent coastal water. State parameters (temperature, salinity and DO) were continuously measured by HOBO Spot (Onset) loggers.

Microbial assemblage analyses: Microbial assemblages inhabiting body wall samples (i.e. biopsy punch; wasting in the absence of external stimuli), lesion margins (i.e epidermal scrapes; wasting in the absence of external stimuli), and at the animal/water interface (i.e. swabs; suboxic and OM enrichment experiments) were examined by 16S rRNA amplicon sequencing (Caporaso et al. 2011). Viral assemblages were examined from the August 2018 study of wasting

progression in the absence of external stimuli by viral metagenomics (Thurber et al. 2009) targeting RNA viruses.

Bacterial cultivation and growth rates: We sought to determine the growth characteristics of asteroid-associated bacteria on organic matter substrates. We isolated three cultures of bacteria, representing common orders retrieved during microbial assemblage analyses, on media containing filtered asteroid tissue homogenates as nutritional source, and examined their growth dynamics on dissolved OM (DOM) from a *Dunaliela tertiolecta* culture, filtered (< 0.7 µm) asteroid tissue homogenates, peptone and glucose at ambient and elevated temperatures.

Association of wasting susceptibility with rugosity and surface area to volume ratio: The relative rugosity between wasting-affected and less wasting-affected asteroid species was examined by imaging approaches. Whole specimens of 11 asteroid species were collected at 3 locations, preserved in 10% neutral buffered formalin, and transported to the College of Veterinary Medicine at Cornell University where they were subject to large animal computed tomography. This analysis provided the total surface area and volume of specimens to a resolution of 400 µm. We also performed micro-computed tomography of ray sections on a subset of these specimens, which provided resolution to 20 µm. The rugosity, surface area, surface area:volume and calculated potential diffusion rates were compared with wasting susceptibility and speed during aquarium studies.

Asteroid specimen respiration: The respiration rates of individual asteroids was measured upon experiment initiation for *Asterias forbesi* and *Pisaster ochraceus* (as described above), and for additional field-collected asteroid species at the Bodega Marine Laboratory. DO depletion was measured in water-tight chambers from which bubbles were eliminated, and recirculated using submersible DC motors. DO depletion rate for each specimen was standardized by specimen mass.

Time series analyses of wasting intensity and chlorophyll a at Whidbey Island: To understand the relationship between ambient primary producer biomass (chlorophyll a), physico-chemical parameters (temperature, salinity, DO), and occurrence of wasting, we examined data obtained from the Penn Cove Shellfish data buoy and compared this to observations of wasting frequency at Coupeville Wharf and Langley Harbor as reported previously (Hewson et al. 2018) from August 2014 to June 2019. We compared the mean time of wasting occurrence over the 5 year

period with mean oceanographic parameters for the period, and also compared the 3 month window before wasting onset with non-wasting months.

Stable isotopic signatures in historical wasting asteroid specimens: The natural abundance of ^{15}N and ^{13}C was determined in 71 individual starfish specimens, including 50 individuals representing paired asymptomatic/wasting affected species at distinct sites and sampling times which were collected as part of prior work during wasting mass mortality (2013-2014).

RESULTS AND DISCUSSION

Shifts in heterotrophic bacterial and archaeal communities during wasting progression reflect oxygen depletion in boundary layers

We observed changes in microbial communities during wasting in the absence of external stimuli and in perturbation experiments that reflect progressive depletion of oxygen at and near the animal/water interface. Time-course analyses of microbiome variation during wasting progression were examined by 16S rRNA amplicon sequencing (Caporaso et al. 2011) (*Supplemental Information; SI*). The relative abundance of taxa within asteroid-associated microbiomes varied with sample type. Body wall (i.e. using a biopsy punch) and epidermis of lesion margin (i.e. scrape on margin) assemblages were dominated by orders Spirochaetales and Cytophagales, while assemblages immediately above and on surfaces (collected by swabs), bore a large proportion of orders associated with organic rich environments, e.g., Alteromonadales, Flavobacteriales, Rhizobiales, and Rhodobacterales (see *Supplemental Information*; *SI*). We observed a progressive increase in copiotrophic orders preceding wasting, including Campylobacterales, Flavobacteriales and Vibrionales (Fig. 1A). This occurred concomitant with an increase in *Nitrosopumilus* and obligate anaerobes (Deltaproteobacteria) relative to a large clade of typically fast-growing phyla (Alpha-and Gammaproteobacteria) immediately prior to lesion genesis (Fig. 1B-D). Following lesion genesis, we observed a further increase in copiotrophs in body wall and epidermal samples, and a proliferation in microaerophiles (*Arcobacter* spp.), facultative anaerobes (*Moritella* spp.) and obligate anaerobic families (Clostridia, Fusobacteria and Bacteroidia) at time of death (Fig. 1A). Collectively, these

178 observations reflect an increasingly anaerobic environment at the epidermal boundary layer
179 which is established prior to wasting onset.

180 Several studies have observed the proliferation of copiotrophic taxa longitudinally during
181 wasting, including genera within the families Flavobacteriaceae, Rhodobacteriacaea (Lloyd and
182 Pespeni 2018), Actinobacteria, and genera in the orders Altermonadales (Nuñez-Pons et al.
183 2018), Vibrionales and Oceanospiralles (Høj et al. 2018). These taxonomic groups are amongst
184 the most active constituents of bacterioplankton and major players in marine organic matter
185 (OM) degradation, some of which have facultative anaerobic metabolisms (Buchan et al. 2014;
186 Choi et al. 2010; Pinhassi et al. 2004; Pohlner et al. 2019; Thiele et al. 2017). While it is
187 tempting to ascribe pathogenicity traits to groups that are enriched on disease-affected tissues
188 (based on members of the same family or genus causing pathology), or infer their role in
189 community dysbiosis (i.e. the microbial boundary effect), this is not possible in the absence of
190 demonstrated pathogenicity or strain-level assignment (Hewson 2019). Previous study
191 comparing wasting and asymptomatic asteroid-associated community gene transcription noted
192 the increase in transcripts from *Propionibacterium*, *Lachnospiraceae* and *Methanosarcina*,
193 which are strict anaerobes, as well as *Stigmatella* and *Staphylococcus*, which are facultative
194 anaerobes, as a proportion of total transcripts (Gudenkauf and Hewson 2015).

195 Taken together, these data suggest that the proliferation of copiotrophic taxa near wasting
196 asteroid surfaces may lead to suboxic conditions at the animal-water interface. All aquatic
197 surfaces are coated with a thin film of water (i.e. diffusive boundary layer) that impedes gas and
198 solute exchange, and, provided aerobic respiration is sufficiently high, suboxic conditions can
199 form on a surface despite oxygen saturated water circulating above (Jørgensen and Revsbech
200 1985). This may result in the proliferation of facultative and obligate anaerobes until asteroid
201 death, and also explains why we observed both an increase in both strict aerobes and strict
202 anaerobes concomitantly. Stimulation of bacteria and subsequent O_2 diffusion limitation is well
203 described in mammalian respiratory systems as well, and is especially pronounced in cystic
204 fibrosis patients. Heterotrophic bacteria inhabiting mammalian lungs thrive on mucins and
205 generate biofilms which further restrict O_2 diffusion into tissues. O_2 consumption by biofilms
206 and by neutrophils may result in hypoxia and reduced diffusion of O_2 across alveolar tissues (Wu
207 et al. 2018). This in turn leads to the proliferation of anaerobes, which are present in clinically

normal lungs (reviewed in (Guilloux et al. 2018) and elevated in diseased lungs (Denner et al. 2016; Spence et al. 2020; Wang et al. 2019). This phenomenon is also observed in fish gills (Legrand et al. 2018; Meyer et al. 2019) which are inhabited by copiotrophic and potentially facultatively anaerobic taxa (Reverter et al. 2017; Rosado et al. 2019).

We found no consistent association between any virus and wasting between specimens, despite increased richness of viruses late in the wasting progression, possibly due to generalized hypoxia-induced replication (*SI*). Moreover, our observations support earlier observation that the Sea Star associated Densovirus (SSaDV; ICTV: Asteroid ambidensovirus 1) is not associated with wasting in any asteroid (Hewson et al. 2018a).

Asteroid wasting is induced by suboxic conditions

Our data demonstrate that SSW is induced by suboxic water column conditions. We incubated *A. forbesi* in suboxic water and observed patterns of wasting progression, boundary layer bacterial abundance and microbial assemblage β-diversity. Dissolved oxygen (DO) concentrations were controlled in an aquarium setting by continuous sparging with N_2, which were on average 39% lower than untreated control incubations (*SI*). All individuals remained asymptomatic in control incubations over the 13 day experiment, while 75% of individuals in hypoxic conditions developed lesions (mean time to lesion genesis = 9.58 ± 0.89 d). Development of lesions over time was strongly related to treatment ($p = 0.006$, log-rank test, df=12). Bacterial abundance on animal surfaces (which we define as abundance in surface samples) corrected for aquarium water values increased in both control and suboxic treatments over the first 6d of incubation, but by day 13, abundance of bacteria in suboxic treatments was significantly lower ($p<0.001$, Student's t-test, df=12) on suboxic treated individuals than in control individuals (Fig. 2). *Asterias forbesi* treated with suboxic waters demonstrated consistent shifts in microbial communities with treatment (*SI*). However, no single bacterial taxonomic organization strongly differentiated normoxic from suboxic conditions.

Wasting induction in *Asterias forbesi* by suboxic conditions is also consistent with our observation that wasting in *Pisaster ochraceus* was inversely correlated to mean flow rate in aquarium studies (i.e. longer residence time of water; *SI*). While we did not measure DO concentrations in flow-rate experiments, lower flow rates into aquaria likely led to faster O_2 depletion and the accumulation of toxic exudates (notably NH_3 [Propp et al. 1983] and S^-

[Vistisen and Vismann 1997]), and establishment of more extensive boundary layer conditions than those individuals incubated in faster flow rates (Fonseca and Kenworthy 1987). The mechanism by which asteroids are particularly sensitive to ambient O_2 concentrations is not well constrained by empirical studies, especially as it relates to SSW. Asteroids mostly rely on passive respiration (c.f. ventilation) and gas diffusion across outer membranes to meet respiratory demand, a point illustrated by mass mortality events of benthic invertebrates, including asteroids, correlated to low O_2 conditions (reviewed in Diaz and Rosenberg 1995; Levin 2003; Levin et al. 2009). Together, these data point to significant influence of O_2 conditions on asteroid wasting. While water column hypoxia events were not observed in concert with SSW in 2013 and beyond, spatially localized hypoxia may occur near surfaces experiencing limited hydrodynamic flow (Gregg et al. 2013).

Organic matter amendment stimulates boundary layer microorganisms and causes rapid wasting

We sought to examine the impact of elevated heterotrophic bacterial respiration on animal surfaces through challenge with various sources of organic matter (OM) which we hypothesized would fuel microbial remineralization. We performed laboratory experiments in which *P. ochraceus* was amended with peptone, *Dunaliella tertiolecta*-derived particulate OM (POM), and coastal seawater POM and examined their impacts on SSW progression and boundary layer bacterial abundance and composition. The addition of organic substrates (peptone and *Dunaliella tertiolecta*-derived POM) induced significantly faster lesion genesis than control incubations ($p=0.012$ for peptone and $p=0.04$ for *Dunaliella*-POM, Student's t-test, $df=5$), but lesion genesis time was not significantly different for the addition of coastal-POM (Fig. 3). Collective treatment temporal pattern of lesion genesis was only significantly different from controls with amendment with peptone ($p = 0.0154$, log-rank test, $df=5$) and *Dunaliella*-POM ($p=0.0339$, log-rank test, $df=5$). Variation in dissolved O_2 in incubations varied over the course of the experiment from 9.6 – 10.2 mg L^{-1} and were never under-saturated. Temperature varied from 12 – 14^{o}C, but variation did not correspond with wasting in any treatment.

Bacterial abundance on asteroid surfaces was variable after enrichment with organic substrates. Individuals that did not waste over the course of the experiment maintained abundances of 0.7 – 2.6 x 10^6 cells mL^{-1}, which was enriched 53 to 1743% above bacterioplankton abundances in

incubation treatments (Fig. 4). All three OM additions elevated bacterial abundances relative to their initial values in the first 48h of the incubation. Between 48 and 96 h, dynamics of surface-inhabiting bacteria varied between treatments. Both *Dunaliella*-POM and peptone, despite initial surges in bacterial abundance, strongly decreased before 96 h, while coastal DOM remained higher than initial values throughout the experiments. The decrease in bacterial abundance after initial increase may be evidence of heterotrophic remineralization-fueled O_2 deficit over time on wasting asteroids, similar to the effect observed in our experiments with *Asterias forbesi* incubated in hypoxic water (Fig. 2). Facultative and strict anaerobes generally experience slow growth rates compared to aerobic taxa because it is less energetically efficient to grow on reduced electron acceptors. While standing stock of aquatic bacteria may be higher in anaerobic conditions than in aerobic conditions, population growth rates are typically lower (Cole and Pace 1995).

The boundary layer microbiota of *P. ochraceus* changed over time in all treatments (Figs. 1B-G; *SI*), but the most prominent changes were distinguished by the copiotrophic orders Flavobacteriales and Rhodobacterales, which increased uniformly in both organic matter amended and untreated individuals, indicating that captivity alone induced changes in microbiome composition (Fig. 5). Since bacterial abundance increased dramatically in the first phase of enrichment, we posit that wasting is induced by copiotroph proliferation on animal surfaces. Heterotrophic bacteria in marine environments remineralize OM that originates from autochthonous and allochthonous sources (Amon and Benner 1996; Benner et al. 1992; Ducklow 1983). Among the myriad of OM sources in seawater, phytoplankton-derived OM are highly labile (Ochiai et al. 1980; Ogawa and Tanoue 2003; Thornton 2014). On regional scales, excess phytoplankton-fueled bacterial respiration, caused by eutrophication and enrichment from terrestrial sources and upwelling zones may result in ‘dead zones’ (e.g. Mississippi River Plume, Peruvian upwelling zone, Benguela current; reviewed in Diaz and Rosenberg 2008) and may be exacerbated by seasonal temperature changes (Murphy et al. 2011) and restricted bathymetry (Diaz 2001). However, water column hypoxia has never been observed at sites where asteroids experienced SSW mass mortality. Indeed, many wasting asteroids occurred in well-circulated and intertidal environments (Hewson et al. 2014). We posit that OM amendment stimulates bacterial abundance immediately adjacent to asteroid respiratory surfaces (i.e. within boundary

298 layers) leading to suboxic microzones and ultimately limiting gas diffusion potential (Gregg et
299 al. 2013).

300 Rapid mineralization of dissolved OM by bacteria near asteroids has been noted previously in
301 studies of epidermal amino acid uptake by *Asterias rubrens*, which ultimately led to decreased
302 animal weight (Siebers 1979), and may be responsible for very low ambient DOM
303 concentrations adjacent to asteroids (Siebers 2015). To illustrate the potential for asteroid surface
304 bacteria to rapidly grow on OM, we isolated 3 cultures on solid media containing tissue
305 homogenates as the sole nutritional source, and examined growth characteristics at two
306 temperatures against variable C sources (algal-derived dissolved (i.e. 0.7 µm-filtered) OM,
307 purified asteroid tissue homogenate, peptone and glucose; *SI*). The three cultures included taxa
308 that belonged to orders that were well-represented in amplicon libraries, including a
309 *Rhodobacteria* (Alphaproteobacteria), and two Altermonadales. Bacteria grew faster, with
310 shorter lag times on peptone in all comparisons and on glucose in most comparisons. While there
311 was considerable lag time in the growth of two cultures (SS1 and SS12) on *Dunaliella tertiolecta*
312 and asteroid tissue DOM, which may be due to lower lability of these substrates, the lag time and
313 growth rates of SS6 (most similar to *Glaciecola* sp.; Altermonadales) was much lower than
314 controls, suggesting rapid assimilation of compounds from these sources. *Glaciecola mesophila*
315 was initially isolated from a marine invertebrate (ascidian) and degrades complex carbohydrates
316 produced by algae (Romanenko et al. 2003). These results demonstrate that bacteria inhabiting
317 asteroid surfaces are capable of rapid uptake and regeneration of various organic compounds,
318 including those we hypothesize may lead to hypoxia on animal surfaces. Our observation that
319 lesion genesis time was best explained by initial bacterial abundance in suboxia-experiments and
320 by overall change in bacterial abundance in the first 3 days of incubation in *Pisaster ochraceus*
321 further indicates a key role of heterotrophic bacteria in wasting.

322 Bacterial stimulation and enhanced wasting in asteroids is paralleled by the DDAM (dissolved
323 organic carbon, disease, algae, microorganism) positive feedback loop in tropical corals (Barott
324 and Rohwer 2012; Dinsdale et al. 2008). Coral disease is associated with OM enrichment (David
325 et al. 2006; Smith et al. 2006), some of which originates from sympatric primary producers
326 (Haas et al. 2010; Haas et al. 2011), which in turn are more labile than OM released from the
327 corals themselves (Haas et al. 2016; Nakajima et al. 2018) and results in both elevated bacterial

abundance on coral surfaces (Dinsdale and Rohwer 2011; Haas et al. 2016), and enhanced remineralization rates (Haas et al. 2016). Bacteria at the coral-water interface have higher energetic demands than those in plankton (Roach et al. 2017), and are highly adapted to organic carbon availability in their local environment (Kelly et al. 2014). The spatial scale on which bacteria react to OM is primarily at water-surface interfaces (Brocke et al. 2015). Hypotheses for the mechanism of coral mortality caused by heterotrophic bacteria include disruption in the balance between corals and their associated microbiota (David et al. 2006), introduction of pathogens that have reservoirs on macroalgae (Nugues et al. 2004), or dysbiosis resulting in invasion by opportunistic pathogens (Barott and Rohwer 2012). In black band disease (BBD), DOC released from primary production causes micro-zones of hypoxia which result in production of toxic sulfides, which in turn result in opening of niches for cyanobacteria (Sato et al. 2017). In asteroid wasting, the proliferation of heterotrophic bacteria and wasting disease may be due to any of these effects. It is also interesting to note that some viral genotypes (e.g. Herpesvirus-like sequences) may be present in higher copy number in diseased coral tissues (Thurber et al. 2008), which is similar to our observation of viruses in asteroids during wasting progression (*SI*).

Culture work and experimental challenge with asteroid tissue homogenates in this study (*SI*), and reported previously (Bucci et al. 2017; Hewson et al. 2014), suggest that wasting may also be associated with decomposition of nearby asteroid individuals via assimilation of tissue-derived compounds and subsequent BLODL. We previously isolated heterotrophic bacteria using sea star tissue homogenates as nutritional source (Hewson et al. 2018a). These bacteria include well-known copiotrophic genera, including those also isolated on sea star tissue homogenate-bearing media in this study (*SI*). Enrichment of near-benthic OM pools by wasting-affected individuals may have resulted in the apparent density dependence of wasting observed in 2014 in some populations (Hewson et al. 2014). Indeed, challenge with tissue homogenates by direct injection into coelomic cavities likely enriches within-and near animal organic matter pools, which in turn may stimulate heterotrophic remineralization. Hence, challenge experiments, such as those performed previously (Bucci et al. 2017; Hewson et al. 2014) and in this study, may be a consequence of BLODL induced by organic matter availability (and possibly protein-bearing material). The apparent transmissibility of SSW in field sites is based on observations of density dependence at some sites, along with geographic spread between adjacent sites and through

public aquaria intake pipes (Hewson et al. 2014). These observations may be inaccurately ascribed to transmissible pathogenic microorganisms, since they may also be explained by enrichment of surrounding habitats and through intake pipes of organic matter pools from decaying individuals.

Wasting is related to species rugosity, individual size, and respiratory demand

Inter- and intra-species susceptibility to asteroid wasting is extensively recorded in previous study, including a significant and positive relationship between individual size and wasting (Hewson et al. 2014), and shifts in size structure after wasting from larger to smaller individuals of *Pisaster ochraceus*, which was believed to be due to recruitment of juveniles (Bates et al. 2009; Eisenlord et al. 2016; Kay et al. 2019; Menge et al. 2016). Wasting in 2013-2014 affected > 20 species of asteroid (Hewson et al. 2014), however the magnitude of SSW impact varied between species. Comparison of community structure before and after wasting suggests inter-species variability in wasting mortality. Asteriid taxa (*Pycnopodia helianthoides, Pisaster* spp., and *Evasterias troschelii*) experienced considerable declines in the Salish Sea (Montecino-Latorre et al. 2016; Schultz et al. 2016) and Southeast Alaska (Konar et al. 2019), while *Dermasterias imbricata* maintained or increased in abundance after mass mortality (Eckert et al. 1999; Konar et al. 2019; Montecino-Latorre et al. 2016; Schultz et al. 2016). In the Channel Islands, SSW disproportionately affected Asteriid taxa relative to *D. imbricata* and *Patiria miniata* (Eckert et al. 1999). Inter-species differences in wasting intensity have been noted in citizen science data accumulated by MARINe (Miner et al. 2018). The potential causes of inter- and within-species wasting susceptibility remain poorly constrained.

We hypothesized that wasting susceptibility may relate to both inter-species variation in rugosity (i.e. degree of corrugation), which dictates diffusive boundary layer thickness, and intra-species surface area-to-volume ratio, which determines total gas flux potential, which are ultimately reflected in patterns of population change since 2013 (Eckert et al. 1999; Montecino-Latorre et al. 2016). Mean and turbulent flow structure around aquatic animals and plants relates to the mean height, density and shape of structures as they compare to flat surfaces (Brodersen et al. 2015; Koch 1994; Nepf 2011). Asteroid surfaces bear numerous spines and processes, including papulae, spines, paxillae and pedicellaria. These structures impart rugosity and thus generate diffusive boundary layers proportional to their relative height under both mean and turbulent

flow. For example, the boundary layer height above the urchin *Evechinus chloroticus.* can be 4-5 mm under low (1.5 cm s^{-1}) flow conditions, which was approximately 2 – 6 X greater than sympatric macroalgae (Hurd et al. 2011). We also speculate that more extensive boundary layers may result in greater entrapment of settled OM from overlying waters. Direct measurement of oxygen concentration in boundary layers as they relate to bacterial remineralization are precluded by the sensitivity of instruments (e.g. microelectrodes) to physical damage in non-immobilized specimens.

To explore the relationship between species rugosity and wasting susceptibility, we examined specimens of similar size (n = 26 individual specimens) representing wasting-affected (n=3) and less/not affected species (n = 5) using whole-animal computed tomography (*SI*). The mean rugosity (defined as 3D:2D surface area) was significantly ($p = 0.015$, Student's t-test, $df = 14$) lower in less affected species than more affected species (Fig. 6). Surface area:volume, individual specimen mass, and overall surface area were not significantly different between categories among similarly-sized animals. Because analysis of large animal specimens is limited to a resolution of 400 µm (which is potentially larger than fine-scale features, e.g. papulae on echinoderm surfaces), we performed further analysis on rays of a subset (n = 16) of individuals using micro-computed tomography, which has a resolution of 20 µm (*SI*). The rugosity of wasting-affected taxa was significantly ($p = 0.0002$, Student's t-test, $df = 4$) greater than less-wasting affected species (Fig. 6). Our observation that more rugose species were more affected by wasting supports the idea that these individuals may be more susceptible because of their greater extent (physical distance) of diffusive boundary layers on respiratory surfaces.

Much of the intra-species wasting susceptibility may also be explained by inherent variation in diffusive flux potential. We observed a significant and positive relationship between wasting lesion genesis rate and animal mass. Larger individuals have a much lower surface area:volume ratio, where surface area is related to gas flux potential. Under near-surface hypoxic conditions, or when diffusion is impeded by extensive boundary layers, larger individuals are more strongly affected than smaller individuals. We also posit that these observations are the result of more extensive boundary layer height above larger specimens. It is also important to note that ossicle density varies between species (Blowes et al. 2017), and those taxa with lower densities (e.g. *Pycnopodia helianthoides*) were more affected than those with higher densities (e.g. *Pisaster*

ochraceus). Species with lower ossicle densities may be differentially susceptible to wasting since their structure may be broken down faster by microbial decomposition or apoptotic processes.

Wasting risk susceptibility may furthermore result from differential diffusive flux potential compared to respiratory demand. We measured the respiration rate (i.e. oxygen demand) of individuals at the start of each experiment, as well as in individuals of several species that were both affected by wasting and those that were less or not affected by wasting that were not a part of experiments to explore whether susceptibility was related to oxygen demand. Mass-normalized measured respiration rates of asteroids were greatest for *Asterias forbesi*, and least for *Dermasterias imbricata* and *Patiria miniata* (*SI*). Both *Pisaster ochraceus* and *Asterias forbesi* respiration rates were considerably more than for other specimens. Measured respiration rates for entire animals was compared to theoretical maximum diffusion rates into coelomic fluids (hereafter abbreviated RR:TD). RR:TD was greatest in *Asterias forbesi* and *Pisaster ochraceus* (which were both >1 in most specimens) and least in *Patiria miniata* and *Dermasterias imbricata* (which were always < 0.1). The observed RR:TD corresponds with wasting susceptibility. Perturbation of O_2 availability in animal surface boundary layers may skew diffusive flux by elongating diffusive path length or reducing differences in O_2 between tissues and surrounding seawater. Hence, specimens with a higher RR:TD may be more affected by the condition than those with lower RR:TD. We cannot account for variable permeability of outer epidermis between individuals (not measured), and assume that all surface area of asteroids is involved in respiration (which may be over-estimated, since presumably some component of this area comprises mineral structures). Some asteroid species inhabiting typically suboxic environments employ morphological and behavioral strategies to meet O_2 demand, including nidamental cavities (Johansen and Petersen 1971; Nance 1981), cribiform organs (Shick et al. 1981), epiproctoral cones (Shick 1976), active ventilation of burrows and decreased size of internal organs (Mironov et al. 2016). However, it is unlikely asteroids typically occurring in normoxic intertidal or subtidal conditions have the ability to morphologically adapt to hypoxic conditions.

Wasting in a field population follows variation in primary production

BLODL-induced wasting in the field may be fueled by several potential allochthonous and autochthonous sources of OM. We hypothesize there are two primary sources fueling BLODL: OM from primary production (phytoplankton and macroalgae), and OM from decaying asteroids. Most asteroid wasting is reported in late fall or summer, with fewer reports during other times of the year (Bates et al. 2009; Eckert et al. 1999; Eisenlord et al. 2016; Harvell et al. 2019; Hewson et al. 2018a; Hewson et al. 2019; Menge et al. 2016; Miner et al. 2018; Montecino-Latorre et al. 2016). We propose that wasting is associated with peak or post-peak declines in phytoplankton production in overlying waters, which subsequently results in peak dissolved OM availability. The mean time of wasting mass mortality observed at Langley and Coupeville, Whidbey Island, fell at or within 1 month after the mean annual maximum of chlorophyll a, minimum DO concentration, maximum temperature, and minimum rainfall (Fig. 7). Multiple linear regression (stepwise, backwards selection criteria) revealed a significant model (R^2=0.866; p=0.001) where temperature (p = 0.006), chlorophyll a (p = 0.027) and salinity (p = 0.044) explained most variation in wasting mass mortality, while forward selection (R^2=0.774; p=0.0002) revealed that monthly variation in wasting was significantly explained by DO alone. Mass mortality was significantly related (one-way ANOVA, p<0.0001) to elevated chlorophyll in the previous 3 months relative to non-mass mortality months, to elevated salinity, and reduced rainfall (*SI*). Phytoplankton in the Puget Sound demonstrate variability in peak productivity by location. In our analysis, chlorophyll a concentration peaked in the central Puget Sound in August, whereas in other locations peak phytoplankton blooms occur in winter and spring (Horner et al. 2005). In the northern Strait of Georgia, chlorophyll a peaks in April (i.e. Spring Bloom) with secondary fall blooms in late October (Suchy et al. 2019). Phytoplankton blooms and their decay results in hypoxia in Puget Sound waters (Barnes and Collias 1958), where bottom water DO concentrations have decreased for the past decade (Khangaonkar et al. 2018).

The coherence of wasting with primary production in the Salish Sea raises the question of why wasting mass mortality in the northeast Pacific occurred in the 12 month period following June 2013, especially when asteroids normally persist at sites experiencing very high phytoplankton biomass and only experienced wasting in 2014 (e.g. Cape Perpetua, OR; (Leslie et al. 2005). Suchy et al. (2019) observed a prolonged (10 month) period of decreased water column stratification, concomitant with strong predominately southerly winds in fall 2013 and spring 2014 in the northern Strait of Georgia. Remotely sensed chlorophyll a in the region was also

479 higher in the northern and central Strait of Georgia in late 2013 compared to previous 8 years
480 and was marked by a significant increase in mid-2013 (Suchy et al. 2019). Mean precipitation
481 was anomalously lower in mid-summer compared to 1981-2010 means, but then increased
482 dramatically in late September 2013, prior to wasting onset in October (17). Phytoplankton
483 abundance in late 2013 was higher than the 1981-2010 average, where peak biomass occurred in
484 late August (later than previous years) (Moore et al. 2014). Ammonia (NH_3) concentration was
485 lowest at the Seattle Aquarium intake in 2013 compared to previous and subsequent years,
486 presumably a reflection of depletion by phytoplankton uptake (Olsen et al. 2017). Elsewhere,
487 there is evidence that wasting in 2013 – 2014 was tied to elevated primary production. The high
488 pCO_2 but low temperature-wasting positive relationship noted in Oregon indicates that upwelling
489 may have stimulated primary production at this location (Menge et al. 2016). The CALCoFi
490 program observed highest coastal upwelling on record in 2013 in central California during
491 wasting onset (Leising et al. 2014). These observations suggest that primary production intensity
492 and timing in 2013-2014 departed from inter-annual variation in prior years, and has followed
493 seasonal patterns since 2014. The breaking of drought conditions in late 2014 in some locations
494 (Hewson et al. 2014) may also have contributed to SSW by delivering enhanced terrestrial OM
495 to coastal regions. The discontinuous latitudinal emergence of wasting in 2013-2014 and
496 regional apparent longshore sequence of SSW occurrence is consistent with regional and basin-
497 scale patterns of organic matter availability. Nearshore primary production is driven by both
498 groundwater discharge and terrestrial runoff, which positively correlates with previous-year
499 rainfall in coastal regions, as well as regional upwelling (Santoro et al. 2010). The spatial scale
500 of phytoplankton blooms sustained solely by terrestrial runoff and groundwater discharge ranges
501 from 880-3600 km^2 in the Southern California Bight (Santoro et al. 2010). Assuming these
502 blooms are constrained within 10 km of shore, the areal extent of phytoplankton-derived organic
503 matter inputs is well within the reported longshore spread of SSW (Hewson et al., 2014).
504 Upwelling, on the other hand, may affect wider coastal productivity patterns. In 2013, strong
505 upwelling was recorded between 36^{o}N and 48^{o}N (i.e. 1,332 km). Thus, the apparent density-
506 dependent local occurrence, and regional spatio-temporal occurrence of SSW is consistent with
507 spatial variation in decaying asteroid and primary production organic matter. It is interesting to
508 note that mass mortality in *Heliaster kubiniji* in the Gulf of California occurred during a
509 prolonged period of heavy rainfall and elevated temperatures prior to El Niño (Dungan et al.

1982). Such rainfall may have caused elevated terrestrial discharge, which in turn may have fueled primary production.

Wasted asteroids in 2013-2017 bore stable isotopic signatures of anaerobic processes

Because wasting has no pathognomic signs and has been reported for over a century (reviewed in Hewson et al., 2018), an obvious question is whether BLODL was related to asteroid mass mortality observed from 2013. While retrospective analyses of O_2 status of asteroids during this event is not possible, hypoxic conditions impart elemental signatures in tissues of preserved specimens. We examined the natural abundance of stable isotopes comparing wasting-affected and grossly normal individuals at the same location and time, in 2013 and 2014. Wasting asteroids (including *Pisaster ochraceus*, *Pycnopodia helianthoides*, and *Evasterias troschelii*), had generally higher $\delta^{15}N$ in their tissues than asymptomatic tissues at the same site within-species (ns) except for *Leptasterias* sp., which had significantly lower $\delta^{15}N$ in wasting tissues than in asymptomatic individuals (Fig. 8). On average between species, $\delta^{15}N$ was enriched by 3.9 ± 3.3 % (7.0 ± 2.8 % excluding *Leptasterias* sp.) in wasted compared to asymptomatic stars. Ellipse analysis, which can be used to infer isotopic niches or metabolic differences between populations (Jackson et al. 2011) suggested that in all paired site-species comparisons wasted stars have altered C and N metabolisms compared to asymptomatic individuals (*SI*). The elemental composition of asteroids, like all animals, largely reflects nutritional source, who obtain anabolic material from consumed prey. Furthermore, asteroids may take up DOM directly from the water column and use these materials for soft body parts, like tube feet (Ferguson 1967a; Ferguson 1967b). The half-life of isotopic signatures in tissues relates to tissue turnover and is most stable in ectotherms (Vander Zanden et al. 2015). Dissimilatory anaerobic nitrogen cycling processes, such as denitrification, shift the balance between ^{15}N and ^{14}N (i.e. selecting against ^{15}N), resulting in higher $\delta^{15}N$ (ratio of tissue ^{15}N to atmospheric ^{15}N) in environments. Thus, we restricted our analysis of tissue $\delta^{15}N$ to fast-growing, regenerative tube feet which will therefore reflect the most recent environmental conditions prior to collection. Translocation of consumed elements to growing tissues is accomplished through continual flux from digestive glands to these tissues through coelomic fluid (Ferguson 1964). Internal tissues of asteroids are inhabited by a suite of bacteria and archaea (Jackson et al. 2018) including abundant spirochaetes

(Holland and Nealson 1978; Kelly et al. 1995; Kelly and McKenzie 1995; Nakagawa et al. 2017). Hence, asteroid tube feet tissues, which are distal from digestive glands, may be influenced by heterotrophic microbial activities which enrich for ^{15}N over ^{14}N. Our finding of higher $\delta^{15}N$ in most wasted asteroids supports the hypothesis that wasting is associated with enhanced anaerobic dissimilatory respiration of nitrogen species, perhaps during translocation of materials between organs or tissues within asteroids, (Ferguson 1964) or during uptake of enriched ^{15}N in DOM pools surrounding affected asteroids (Ferguson 1967a; Ferguson 1967b).

To the best of our knowledge, there has only been one previous report on the effects of hypoxia on stable isotopic composition in animal tissues. Oysters affected by hypoxic water conditions demonstrated $\delta^{15}N$ enrichment, which they propose was due to hypoxia-induced starvation responses resulting in recycling of internal tissues (Patterson and Carmichael 2018). Asteroids likewise have similar autophagous responses to starvation, prioritizing somatic maintenance over reproduction (Aquinas and Nimitz 1976; Harrold and Pearse 1980). Under typical food availability, reproductive and digestive tissues demonstrate inverse relationships in overall size relating to spawning and feeding time in most asteroid species. However, the ratio between reproductive and digestive tissues in *Leptasterias* spp. is synchronous over time in females (but not so in males), which is different from other starfish species (Menge 1975). We speculate that the lower $\delta^{15}N$ observed in wasting *Leptasterias* spp., an opposite trend to other species, may relate to timing of autophagous transfer of materials within individuals and timing of predicted hypoxia (which peaks in late summer) relative to autophagy within animals. It is also possible that asymptomatic and wasting affected specimens were different species of *Leptasterias* sp. since they form a cryptic species complex (Melroy et al. 2017), which may affect comparison between disease states.

Further evidence for BLODL association with wasting

Wasting imparts transcriptional and population genetic changes in asteroids and surviving populations, respectively. In studies comparing gene expression between wasting and asymptomatic individuals, the relative transcription of high affinity cytochrome c oxidase (ccb3; (Preisig et al. 1996) was higher in symptomatic individuals (Gudenkauf and Hewson 2015). Furthermore, cytochrome P450 2J6, which plays a dual role in both oxidation and detoxification of H_2S (Tobler et al. 2014), was expressed in at least two studies of wasting asteroids (Fuess et

al. 2015; Gudenkauf and Hewson 2015). Surviving juvenile recruits are genetically distinct to asteroids before 2013 (Schiebelhut et al. 2018). Loci selected for in surviving populations correspond to those heightened in experiments with elevated temperature (Ruiz-Ramos et al. 2020). In particular, Ruiz-Ramos et al (2020) found a synchronous decrease in expression of ND5 (NADH dehydrogenase 5) among field-wasting specimens and those subject to temperature challenge in aquaria, and corresponding mutation in ND5 in surviving populations. Extracellular hypoxia causes downregulation of NADH dehydrogenase in vertebrate cells (Piruat and López-Barneo 2005), and variation in mt ND5 genes is related to hypoxia sensitivity in humans (Sharma et al. 2019). Elevated temperatures may reduce overall O_2 concentrations in seawater and cause faster microbial growth rates. Our asteroid associated bacterial culture experiments illustrate faster growth rates and shorter lag times in OM uptake under warmer conditions. Hence, previous observations of enhanced temperature corresponding to wasting (Eisenlord et al. 2016; Harvell et al. 2019; Kohl et al. 2016; Miner et al. 2018; Montecino-Latorre et al. 2016) and with periodic temperature excursion frequency (Aalto et al. 2020) are consistent with the BLODL model proposed in our work.

Conclusion

Here we present evidence to support our hypothesis that wasting is a sequela of BLODL. We provide evidence that this condition may relate to bacterial abundance/compositional shifts on asteroid respiratory surfaces, and that this likely results from enrichment with OM. In natural conditions, this corresponds with seasonal patterns of water column productivity, and in controlled experiments we demonstrate that algal-derived OM stimulates wasting and OM release from animal tissues. We also provide evidence for this effect as occurring in specimens from the 2013 – 2014 mass mortality event. Our results suggest that wasting via this mechanism may be exacerbated under warmer ocean conditions, or conditions in which labile OM from terrestrial sources (which may include anthropogenic nutrient pollution) may be present in coastal environments. Holothurian wasting, bearing similarity to asteroid wasting in gross disease signs, was anecdotally reported in the Puget Sound and southeast Alaska beginning in 2015 (Jackson et al. 2016). Most urchin diseases are associated with diverse bacteria capable of anaerobic metabolism (reviewed in Hewson 2019). Hence, BLODL may help explain the

599 variation in etiologies observed between echinoderms and between other invertebrate groups,
600 especially those that rely on diffusion for respiratory activities.

601 **ACKNOWLEDGEMENTS**

602 The authors are grateful to Jim Nagel (Penn Cove Shellfish Company), Karl Menard (Bodega
603 Bay Marine Laboratory), Taylor White (UC Santa Cruz), Joe Gaydos, Lizzy Ashley (Seadoc
604 Society), Martin Haulena (Vancouver Aquarium), Lesanna Lahner (Minnesota Zoo) and Kipp
605 Quinby for provision of specimens and data; Betsy Steele (UC Santa Cruz), Joel Markis and
606 Marnie Chapman (University of Alaska Southeast) for use of laboratory space; Kim Sparks and
607 Elliot Jackson (Cornell University) for laboratory assistance; M. Sewell (U Auckland),
608 Christopher Mah (Smithsonian) and Thierry Work (USGS) for assistance with experiments and
609 comments on an early manuscript draft. Asteroid collections were performed under permits CF-
610 19-107 from the Alaska Department of Fish and Game, 19-149a from the Washington State
611 Department of Fish and Wildlife and SC-13144 from the California Department of Fish and
612 Wildlife. This work was supported by US National Science Foundation Grants OCE-1537111
613 and OCE-1737127 awarded to IH and USGS Contract G19AC00434 awarded to IH and T.
614 Work.

615

616 **References**

617 Aalto, E. A. and others 2020. Models with environmental drivers offer a plausible mechanism for
618 the rapid spread of infectious disease outbreaks in marine organisms. Sci Rep **10:** 5975.
619 Amon, R. M. W., and R. Benner. 1996. Bacterial utilization of different size classes of dissolved
620 organic matter. Limnol Oceanogr **41:** 41-51.
621 Aquinas, S. M., and O.P. Nimitz. 1976. Histochemical changes in gonadal nutrient reserves
622 correlated with nutrition in the sea stars *Pisaster ochraceus* and *Patiria miniata*. Biol Bull
623 **151:** 357-369.
624 Barnes, C. A., and E. E. Collias. 1958. Some considerations of oxygen utilization rates in Puget
625 Sound. J Mar Res **17:** 68-80.
626 Barott, K. L., and F. L. Rohwer. 2012. Unseen players shape benthic competition on coral reefs.
627 Trends in Microbiology **20:** 621-628.
628 Bates, A. E., B. J. Hilton, and C. D. G. Harley. 2009. Effects of temperature, season and locality
629 on wasting disease in the keystone predatory sea star *Pisaster ochraceus*. Dis Aquat Org
630 **86:** 245-251.

631 Benner, R., J. D. Pakulski, M. McCarthy, J. I. Hedges, and P. G. Hatcher. 1992. Bulk chemical
632 characteristics of dissolved organic matter in the ocean. Science **255:** 1561-1564.
633 Blowes, L. M. and others 2017. Body wall structure in the starfish *Asterias rubens*. J Anat **231:**
634 325-341.
635 Brocke, H. J., L. Polerecky, D. de Beer, M. Weber, J. Claudet, and M. M. Nugues. 2015. Organic
636 matter degradation drives benthic cyanobacterial mat abundance on Caribbean coral
637 reefs. PLoS One **10:** e0125445.
638 Brodersen, K., M. Lichtenberg, L.-C. Paz, and M. Kühl. 2015. Epiphyte-cover on seagrass
639 (*Zostera marina* L.) leaves impedes plant performance and radial O_2 loss from the below-
640 ground tissue. Front Mar Sci **2**. https://doi.org/10.3389/fmars.2015.00058
641 Bucci, C. and others 2017. Sea star wasting disease in *Asterias forbesi* along the Atlantic Coast
642 of North America. PLoS One **12:** 20.
643 Buchan, A., G. R. LeCleir, C. A. Gulvik, and J. M. González. 2014. Master recyclers: features
644 and functions of bacteria associated with phytoplankton blooms. Nat Rev Microbiol **12:**
645 686-698.
646 Caporaso, J. G. and others 2011. Global patterns of 16S rRNA diversity at a depth of millions of
647 sequences per sample. Proc Nat Acad Sci USA **108:** 4516-4522.
648 Choi, E. J., H. C. Kwon, Y. C. Sohn, and H. O. Yang. 2010. *Kistimonas asteriae* gen. nov., sp.
649 nov., a gammaproteobacterium isolated from *Asterias amurensis*. Int J System Evol
650 Microbiol **60:** 938-943.
651 Cole, J. J., and M. L. Pace. 1995. Bacterial secondary production in oxic and anoxic freshwaters.
652 Limnol Oceanogr **40:** 1019-1027.
653 David, I. K., M. K. Neilan, B. Mya, K. Nancy, and R. Forest. 2006. Role of elevated organic
654 carbon levels and microbial activity in coral mortality. Mar Ecol Progr Ser **314:** 119-125.
655 Denner, D. R. and others 2016. Corticosteroid therapy and airflow obstruction influence the
656 bronchial microbiome, which is distinct from that of bronchoalveolar lavage in asthmatic
657 airways. J Allerg Clin Immunol **137:** 1398.
658 Diaz, R. J. 2001. Overview of hypoxia around the world. J Environ Qual **30:** 275-281.
659 Diaz, R. J., and R. Rosenberg. 1995. Marine benthic hypoxia: A review of its ecological effects
660 and the behavioural responses of benthic macrofauna. Oceanogr Mar Biol Ann Rev **33:**
661 245-303.

662 ---. 2008. Spreading dead zones and consequences for marine ecosystems. Science **321:** 926-929.
663 Dinsdale, E. A. and others 2008. Microbial ecology of four coral atolls in the Northern Line
664 Islands. PLoS One **3:** e1584.
665 Dinsdale, E. A., and F. Rohwer. 2011. Fish or germs? Microbial dynamics associated with
666 changing trophic structures on coral reefs, p. 231-240. *In* Z. Dubinsky and N. Stambler
667 [eds.], Coral Reefs: An Ecosystem in Transition. Springer Netherlands.
668 Ducklow, H. W. 1983. Production and fate of bacteria in the oceans. Bioscience **33:** 494-501.
669 Dungan, M. L., T. E. Miller, and D. A. Thomson. 1982. Catastrophic decline of a top carnivore
670 in the Gulf of California rocky intertidal zone. Science **216:** 989-991.
671 Eckert, G., J. M. Engle, and D. Kushner. 1999. Sea star disease and population declines at the
672 Channel Islands, p. 435-441. 6th California Islands Symposium.
673 Eisenlord, M. E. and others 2016. Ochre star mortality during the 2014 wasting disease
674 epizootic: role of population size structure and temperature. Phil Transact Roy Soc B
675 **371:** 20150212.
676 Ferguson, J. C. 1964. Nutrient transport in starfish. I. Properties of the coelomic fluid. Biol Bull
677 **126:** 33-53.
678 ---. 1967a. An autoradiographic study of the utilization of free exogenous amino acids by
679 starfishes. Biol Bull **133:** 317-329.
680 ---. 1967b. Utilization of dissolved exogenous nutrients by the starfishes, *Asterias forbesi* and
681 *Henricia sanguinolenta*. Biol Bull **132:** 161-173.
682 Fonseca, M. S., and W. J. Kenworthy. 1987. Effects of current on photosynthesis and distribution
683 of seagrasses. Aquat Bot **27:** 59-78.
684 Fuess, L. E. and others 2015. Up in arms: Immune and nervous system response to sea star
685 wasting disease. PLoS One **10:** e0133053.
686 Gregg, A. K. and others 2013. Biological oxygen demand optode analysis of coral reef-
687 associated microbial communities exposed to algal exudates. PeerJ **1:** e107.
688 Gudenkauf, B. M., and I. Hewson. 2015. Metatranscriptomic analysis of *Pycnopodia*
689 *helianthoides* (Asteroidea) affected by sea star wasting disease. PLoS One **10:** e0128150.
690 Guilloux, C. A., C. Lamoureux, and G. Hery-Arnaud. 2018. Anaerobic bacteria, the unknown
691 members of the lung microbiota. Med Sci **34:** 253-260.
692 Haas, A. F. and others 2016. Global microbialization of coral reefs. Nature Microbiol **1:** 16042.

693 Haas, A. F., M. S. Naumann, U. Struck, C. Mayr, M. el-Zibdah, and C. Wild. 2010. Organic
694 matter release by coral reef associated benthic algae in the Northern Red Sea. J Exper
695 Mar Biol Ecol **389:** 53-60.
696 Haas, A. F. and others 2011. Effects of coral reef benthic primary producers on dissolved organic
697 carbon and microbial activity. PLoS One **6:** e27973-e27973.
698 Harrold, C., and J. S. Pearse. 1980. Allocation of pyloric caecum reserves in FED and starved
699 sea stars, *Pisaster giganteus* (Stimpson): Somatic maintenance comes before
700 reproduction. J Exper Mar Biol Ecol **48:** 169-183.
701 Harvell, C. D. and others 2019. Disease epidemic and a marine heat wave are associated with the
702 continental-scale collapse of a pivotal predator *Pycnopodia helianthoides*. Science
703 Advances **5:** eaau7042.
704 Hewson, I. 2019. Technical pitfalls that bias comparative microbial community analyses of
705 aquatic disease. Dis Aquat Organ **137:** 109-124.
706 Hewson, I. and others 2018. Investigating the complex association between viral ecology,
707 environment, and Northeast Pacific sea star wasting. Front Mar Sci **5**.
708 https://doi.org/10.3389/fmars.2018.00077
709 Hewson, I. and others 2014. Densovirus associated with sea-star wasting disease and mass
710 mortality. Proc Nat Acad Sci USA **111:** 17276-17283.
711 Hewson, I. and others 2019. Perspective: Something old, something new? Review of wasting and
712 other mortality in Asteroidea (Echinodermata). Front Mar Sci **6**.
713 https://doi.org/10.3389/fmars.2019.00406
714 Høj, L. and others 2018. Crown-of-thorns sea star *Acanthaster* cf. *solaris* has tissue-
715 characteristic microbiomes with potential roles in health and reproduction. Appl Environ
716 Microbiol **84**. DOI: 10.1128/AEM.00181-18
717 Holland, N. D., and K. H. Nealson. 1978. Fine-structure of the echinoderm cuticle and the sub-
718 cuticular bacteria of echinoderms. Acta Zool **59:** 169-185.
719 Horner, R. A., J. R. Postel, C. Halsband-Lenk, J. J. Pierson, G. Pohnert, and T. Wichard. 2005.
720 Winter-spring phytoplankton blooms in Dabob Bay, Washington. Progr Oceanogr **67:**
721 286-313.

722 Hurd, C. L. and others 2011. Metabolically induced pH fluctuations by some coastal calcifiers
723 exceed projected 22nd century ocean acidification: a mechanism for differential
724 susceptibility? Global Change Biol **17:** 3254-3262.
725 Jackson, A. L., R. Inger, A. C. Parnell, and S. Bearhop. 2011. Comparing isotopic niche widths
726 among and within communities: SIBER - Stable Isotope Bayesian Ellipses in R. J Anim
727 Ecol **80:** 595-602.
728 Jackson, E. W., K. S. I. Bistolas, J. B. Button, and I. Hewson. 2016. Novel circular single-
729 stranded DNA viruses among an asteroid, echinoid and holothurian (Phylum:
730 Echinodermata). PLoS One **11:** e0166093.
731 Jackson, E. W., C. Pepe-Ranney, S. J. Debenport, D. H. Buckley, and I. Hewson. 2018. The
732 microbial landscape of sea stars and the anatomical and interspecies variability of their
733 microbiome. Front Microbiol **9:** 12.
734 Jackson, E. W., C. Pepe-Ranney, M. R. Johnson, D. L. Distel, and I. Hewson. 2020. A highly
735 prevalent and pervasive densovirus discovered among sea stars from the North American
736 Atlantic Coast. Appl Environ Microbiol **86**. DOI: 10.1128/AEM.02723-19
737 Jaffe, N., R. Eberl, J. Bucholz, and C. S. Cohen. 2019. Sea star wasting disease demography and
738 etiology in the brooding sea star *Leptasterias* spp. PLoS One **14:** e0225248.
739 Johansen, K., and J. A. Petersen. 1971. Gas exchange and active ventilation in a starfish,
740 *Pteraster tesselatus*. Zeitschrift für vergleichende Physiologie **71:** 365-381.
741 Jørgensen, B. B., and N. P. Revsbech. 1985. Diffusive boundary layers and the oxygen uptake of
742 sediments and detritus. Limnol Oceanogr **30:** 111-122.
743 Kay, S. W. C., A.-L. M. Gehman, and C. D. G. Harley. 2019. Reciprocal abundance shifts of the
744 intertidal sea stars, *Evasterias troschelii* and *Pisaster ochraceus*, following sea star
745 wasting disease. Proc Roy Soc B **286:** 20182766.
746 Kelly, L. W. and others 2014. Local genomic adaptation of coral reef-associated microbiomes to
747 gradients of natural variability and anthropogenic stressors. Proc Nat Acad Sci USA **111:**
748 10227-10232.
749 Kelly, M. S., M. F. Barker, J. D. McKenzie, and J. Powell. 1995. The incidence and morphology
750 of subcuticular bacteria in the echinoderm fauna of New Zealand. Biol Bull **189:** 91-105.

751 Kelly, M. S., and J. D. McKenzie. 1995. Survey of the occurrence and morphology of sub-
752 cuticular bacteria in shelf echinoderms from the Northeast Atlantic Ocean. Mar Biol **123:**
753 741-756.
754 Khangaonkar, T. and others 2018. Analysis of hypoxia and sensitivity to nutrient pollution in
755 Salish Sea. J Geophys Res Oceans **123:** 4735-4761.
756 Koch, E. W. 1994. Hydrodynamics, diffusion-boundary layers and photosynthesis of the
757 seagrasses *Thalassia testudinum* and *Cymodocea nodosa*. Mar Biol **118:** 767-776.
758 Kohl, W. T., T. I. McClure, and B. G. Miner. 2016. Decreased temperature facilitates short-term
759 sea star wasting disease survival in the keystone intertidal sea star *Pisaster ochraceus*.
760 PLoS One **11:** e0153670.
761 Konar, B. and others 2019. Wasting disease and static environmental variables drive sea star
762 assemblages in the Northern Gulf of Alaska. J Exper Mar Biol Ecol **520:** 151209.
763 Legrand, T. and others 2018. The inner workings of the outer surface: Skin and gill microbiota as
764 indicators of changing gut health in Yellowtail Kingfish. Front Microbiol **8:** 17.
765 Leising, A. W. and others 2014. State of the Caliofornia Current 2013-2014: El Nino Looming.
766 CalCOFI Report **55:** 51-87.
767 Leslie, H. M., E. N. Breck, F. Chan, J. Lubchenco, and B. A. Menge. 2005. Barnacle
768 reproductive hotspots linked to nearshore ocean conditions. Proc Nat Acad Sci USA **102:**
769 10534-10539.
770 Levin, L. A. 2003. Oxygen minimum zone benthos: Adaptation and community response to
771 hypoxia. Oceanogr Mar Biol Ann Rev **41:** 1-45.
772 Levin, L. A. and others 2009. Effects of natural and human-induced hypoxia on coastal benthos.
773 Biogeosciences **6:** 2063-2098.
774 Lloyd, M. M., and M. H. Pespeni. 2018. Microbiome shifts with onset and progression of sea star
775 wasting disease revealed through time course sampling. Sci Rep **8:** 12.
776 Mead, A. D. 1898. Twenty-eighth Annual Report of the Commissioners of Inland Fisheries,
777 Made to the General Assembly at Its January Session, 1898, p. 112. *In* J. M. K.
778 Southwick et al. [eds.].
779 Melroy, L. M., R. J. Smith, and C. S. Cohen. 2017. Phylogeography of direct-developing sea
780 stars in the genus *Leptasterias* in relation to San Francisco Bay outflow in central
781 California. Mar Biol **164**.

Menge, B. A. 1975. Brood or broadcast? The adaptive significance of different reproductive strategies in the two intertidal sea stars *Leptasterias hexactis* and *Pisaster ochraceus*. Mar Biol **31:** 87-100.

Menge, B. A., E. B. Cerny-Chipman, A. Johnson, J. Sullivan, S. Gravem, and F. Chan. 2016. Sea star wasting disease in the keystone predator *Pisaster ochraceus* in Oregon: Insights into differential population impacts, recovery, predation rate, and temperature effects from long-term research. PLoS One **11:** e0153994.

Meyer, J. L., J. Castellanos-Gell, G. S. Aeby, C. C. Häse, B. Ushijima, and V. J. Paul. 2019. Microbial community shifts associated with the ongoing stony coral tissue loss disease outbreak on the Florida Reef Tract. Front Microbiol **10**. doi: 10.3389/fmicb.2019.02244

Miner, C. M. and others 2018. Large-scale impacts of sea star wasting disease (SSWD) on intertidal sea stars and implications for recovery. PLoS One **13:** e0192870.

Mironov, A. N., A. B. Dilman, I. P. Vladychenskaya, and N. B. Petrov. 2016. Adaptive strategy of the Porcellanasterid sea stars. Biol Bull **43:** 503-516.

Montecino-Latorre, D. and others 2016. Devastating transboundary impacts of sea star wasting disease on subtidal asteroids. PLoS One **11:** e0163190.

Moore, S. K., K. Stark, J. Bos, P. Williams, J. Newton, and K. Dzinbal. 2014. Puget sound marine waters: 2013 overview. *In* P. S. E. M. P. M. W. Workgroup [ed.].

Murphy, R. R., W. M. Kemp, and W. P. Ball. 2011. Long-term trends in Chesapeake Bay seasonal hypoxia, stratification, and nutrient loading. Est Coast **34:** 1293-1309.

Nakagawa, S. and others 2017. Microbiota in the coelomic fluid of two common coastal starfish species and characterization of an abundant *Helicobacter*-related taxon. Sci Rep **7:** 8764.

Nakajima, R. and others 2018. Release of dissolved and particulate organic matter by the soft coral Lobophytum and subsequent microbial degradation. J Exper Mar Biol Ecol **504:** 53-60.

Nance, J. M. 1981. Respiratory water flow and production of mucus in the cushion star, *Pteraster tesselatus* Ives (Echinodermata: Asteroidea). J Exper Mar Biol Ecol **50:** 21-31.

Nepf, H. M. 2011. 2.13 - Flow Over and Through Biota, p. 267-288. *In* E. Wolanski and D. McLusky [eds.], Treatise on Estuarine and Coastal Science. Academic Press.

Noble, R. T., and J. A. Fuhrman. 1998. Use of SYBR Green I rapid epifluoresence counts of marine viruses and bacteria. Aquat Microb Ecol **14:** 113-118.

Nugues, M. M., G. W. Smith, R. J. van Hooidonk, M. I. Seabra, and R. P. M. Bak. 2004. Algal contact as a trigger for coral disease. Ecol Lett **7:** 919-923.

Nunez-Pons, L., T. M. Work, C. Angulo-Preckler, J. Moles, and C. Avila. 2018. Exploring the pathology of an epidermal disease affecting a circum-Antarctic sea star. Sci Rep **8:** 12.

Ochiai, M., T. Nakajima, and T. Hanya. 1980. Chemical composition of labile fractions in DOM. Hydrobiol **71:** 95-97.

Ogawa, H., and E. Tanoue. 2003. Dissolved organic matter in oceanic waters. J Oceanogr **59:** 129-147.

Olsen, A. Y., A. Smith, and S. Larson. 2017. A temporal analysis of water quality variability at the Seattle Aquarium in Elliott Bay, Puget Sound, WA, p. 55-69. *In* M. Glavan [ed.], Water Challenges of an Urbanizing World. IntechOpen.

Patterson, H. K., and R. H. Carmichael. 2018. Dissolved oxygen concentration affects δ15N values in oyster tissues: implications for stable isotope ecology. Ecosphere **9:** e02154.

Pinhassi, J. and others 2004. Changes in bacterioplankton composition under different phytoplankton regimens. Appl Environ Microbiol **70:** 6753-6766.

Piruat, J. I., and J. López-Barneo. 2005. Oxygen tension regulates mitochondrial DNA-encoded complex I gene expression. J Biol Chem **280:** 42676-42684.

Pohlner, M., L. Dlugosch, B. Wemheuer, H. Mills, B. Engelen, and B. K. Reese. 2019. The majority of active *Rhodobacteraceae* in marine sediments belong to uncultured genera: A molecular approach to link their distribution to environmental conditions. Front Microbiol **10**. https://doi.org/10.3389/fmicb.2019.00659

Porter, K. G., and Y. S. Feig. 1980. The use of DAPI for identifying and counting aquatic microflora. Limnol Oceanogr **25:** 943-948.

Preisig, O., R. Zufferey, L. Thöny-Meyer, C. A. Appleby, and H. Hennecke. 1996. A high-affinity cbb3-type cytochrome oxidase terminates the symbiosis-specific respiratory chain of *Bradyrhizobium japonicum*. J Bacteriol **178:** 1532-1538.

Propp, M. V., V. I. Ryabushko, A. A. Zhuchikhina, and L. N. Propp. 1983. Seasonal changes in respiration, ammonia and phosphate excretion, and activity of carbohydrate-metabolism enzymes in four echinoderm species from the sea of Japan. Comp Biochem Physiol B **75:** 707-711.

Reverter, M., P. Sasal, N. Tapissier-Bontemps, D. Lecchini, and M. Suzuki. 2017. Characterisation of the gill mucosal bacterial communities of four butterflyfish species: a reservoir of bacterial diversity in coral reef ecosystems. FEMS Microbiol Ecol **93:** 10.

Roach, T. N. F. and others 2017. Microbial bioenergetics of coral-algal interactions. PeerJ **5:** e3423.

Romanenko, L. A., N. V. Zhukova, M. Rohde, A. M. Lysenko, V. V. Mikhailov, and E. Stackebrandt. 2003. *Glaciecola mesophila* sp. nov., a novel marine agar-digesting bacterium. Int J System Evol Microbiol **53:** 647-651.

Rosado, D., M. Pérez-Losada, R. Severino, J. Cable, and R. Xavier. 2019. Characterization of the skin and gill microbiomes of the farmed seabass (*Dicentrarchus labrax*) and seabream (*Sparus aurata*). Aquaculture **500:** 57-64.

Ruiz-Ramos, D. V., L. M. Schiebelhut, K. J. Hoff, J. P. Wares, and M. N. Dawson. 2020. An initial comparative genomic autopsy of wasting disease in sea stars. Molecular Ecology **29:** 1087-1102.

Santoro, A. E., N. J. Nidzieko, G. L. v. Dijken, K. R. Arrigo, and A. B. Boehma. 2010. Contrasting spring and summer phytoplankton dynamics in the nearshore Southern California Bight. Limnol Oceanogr **55:** 264-278.

Sato, Y. and others 2017. Unraveling the microbial processes of black band disease in corals through integrated genomics. Sci Rep **7:** 40455.

Schiebelhut, L. M., J. B. Puritz, and M. N. Dawson. 2018. Decimation by sea star wasting disease and rapid genetic change in a keystone species, *Pisaster ochraceus*. Proc Nat Acad Sci USA **115:** 7069-7074.

Schultz, J. A., R. N. Cloutier, and I. M. Cote. 2016. Evidence for a trophic cascade on rocky reefs following sea star mass mortality in British Columbia. PeerJ **4:** 19.

Sharma, S. and others 2019. Mitochondrial DNA sequencing reveals association of variants and haplogroup M33a2′3 with high altitude pulmonary edema susceptibility in Indian male lowlanders. Sci Rep **9**.

Shibata, A., Y. Goto, H. Saito, T. Kikuchi, T. Toda, and S. Taguchi. 2006. Comparison of SYBR Green I and SYBR Gold stains for enumerating bacteria and viruses by epifluorescence microscopy. Aquat Microb Ecol **43:** 223-231.

873 Shick, J. M. 1976. Physiological and behavioral responses to hypoxia and hydrogen sulfide in the
874 infaunal asteroid *Ctenodiscus crispatus*. Mar Biol **37:** 279-289.
875 Shick, J. M., K. C. Edwards, and J. H. Dearborn. 1981. Physiological ecology of the deposit-
876 feeding sea star Ctenodiscus crispatus - Ciliated surfaces and animal-sediment
877 interactions. Mar Ecol Progr Ser **5:** 165-184.
878 Siebers, D. 1979. Transintegumentary uptake of dissolved amino acids in the sea star Asterias
879 rubens - Reassessment of its nutritional role with special reference to the significance of
880 heterotrophic bacteria. Mar Ecol Progr Ser **1:** 169-177.
881 Siebers, D. 2015. Bacterial—invertebrate interactions in uptake of dissolved organic matter.
882 Amer Zool **22:** 723-733.
883 Silverman J.D., Washburne A.D., Mukherjee S., & David L.A. 2017. A phylogenetic transform
884 enhances analysis of compositional microbiota data. eLife **6**:e21887
885 Smith, J. E. and others 2006. Indirect effects of algae on coral: algae-mediated, microbe-induced
886 coral mortality. Ecol Lett **9:** 835-845.
887 Spence, C. D. and others 2020. Influence of azithromycin and allograft rejection on the post-lung
888 transplant microbiota. J Heart Lung Transplant **39:** 176-183.
889 Suchy, K. D., N. Le Baron, A. Hilborn, R. I. Perry, and M. Costa. 2019. Influence of
890 environmental drivers on spatio-temporal dynamics of satellite-derived chlorophyll a in
891 the Strait of Georgia. Progr Oceanogr **176:** 102134.
892 Thiele, S., M. Richter, C. Balestra, F. O. Glöckner, and R. Casotti. 2017. Taxonomic and
893 functional diversity of a coastal planktonic bacterial community in a river-influenced
894 marine area. Mar Genom **32:** 61-69.
895 Thornton, D. C. O. 2014. Dissolved organic matter (DOM) release by phytoplankton in the
896 contemporary and future ocean. Eur J Phycol **49:** 20-46.
897 Thurber, R. L. V. and others 2008. Metagenomic analysis indicates that stressors induce
898 production of herpes-like viruses in the coral *Porites compressa*. Proc Nat Acad Sci USA
899 **105:** 18413-18418.
900 Thurber, R. V., M. Haynes, M. Breitbart, L. Wegley, and F. Rohwer. 2009. Laboratory
901 procedures to generate viral metagenomes. Nat Protoc **4:** 470-483.

902 Tobler, M., C. Henpita, B. Bassett, J. L. Kelley, and J. H. Shaw. 2014. H_2S exposure elicits
903 differential expression of candidate genes in fish adapted to sulfidic and non-sulfidic
904 environments. Comp Biochem Physiol A **175:** 7-14.
905 Vander Zanden, M. J., M. K. Clayton, E. K. Moody, C. T. Solomon, and B. C. Weidel. 2015.
906 Stable isotope turnover and half-life in animal tissues: A literature synthesis. PLoS One
907 **10:** e0116182.
908 Vistisen, B., and B. Vismann. 1997. Tolerance to low oxygen and sulfide in *Amphiura filiformis*
909 and *Ophiura albida* (Echinodermata: Ophiuroidea). Mar Biol **128:** 241-246.
910 Wang, K. and others 2019. A preliminary study of microbiota diversity in saliva and
911 bronchoalveolar lavage fluid from patients with primary bronchogenic carcinoma. Med
912 Sci Monit **25:** 2819-2834.
913 Washburne A.D., and others. 2017. Phylogenetic factorization of compositional data yields
914 lineage-level associations in microbiome datasets. PeerJ **5**:e2969.
915 Wu, Y., I. Klapper, and P. S. Stewart. 2018. Hypoxia arising from concerted oxygen
916 consumption by neutrophils and microorganisms in biofilms. Pathog Dis **76:** fty043.

917

918

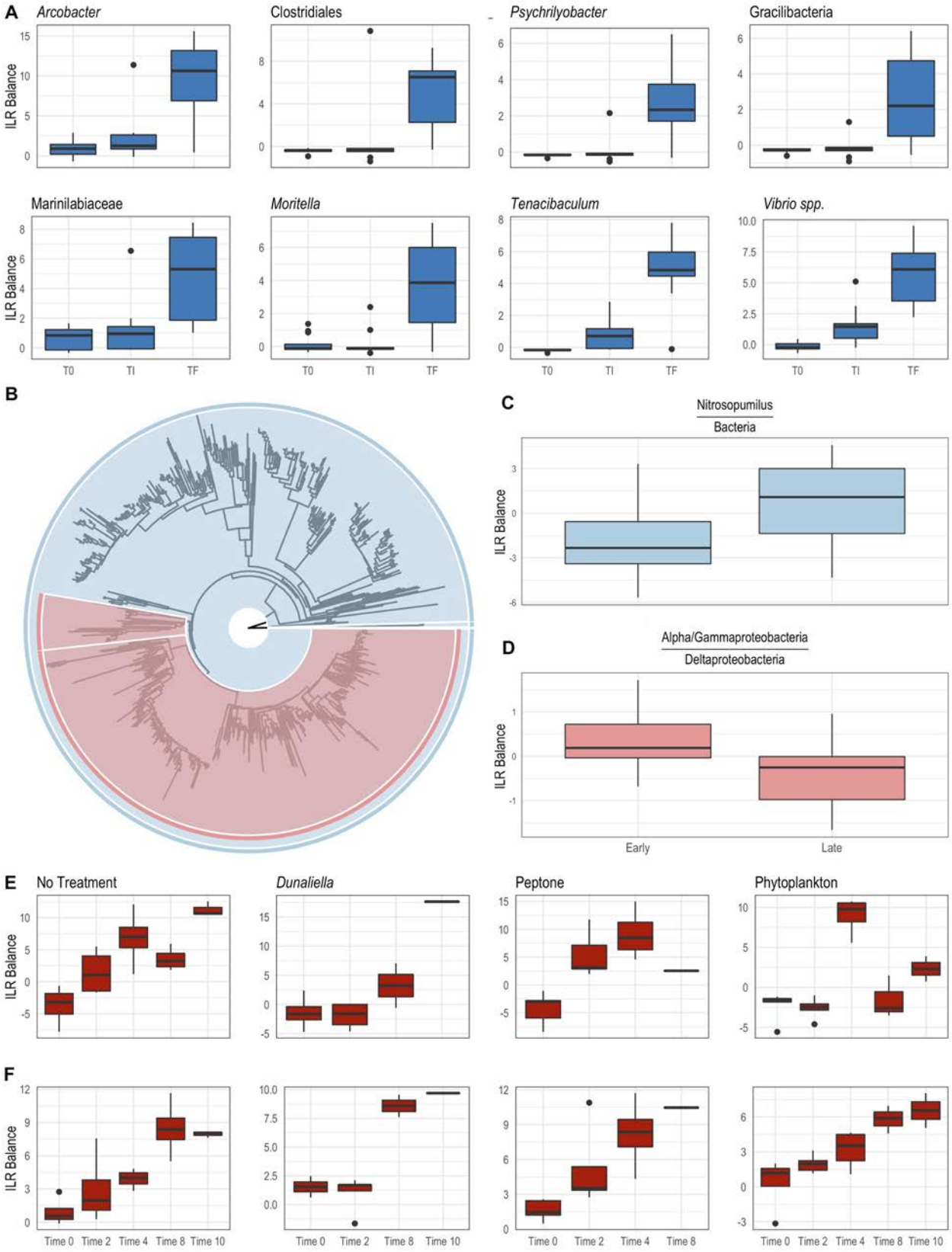

Fig. 1: Differential abundance of bacterial taxa from body wall samples (A; *P. ochraceus* June 2018) and surface swabs (B-F; *P. ochraceus* August 2019). (A) Boxplots were derived using PhyloFactor (Washburne et al. 2017), which uses a generalized linear model to regress the isometric log-ratio (ILR balance) between opposing clades (contrasted by an edge) on a phylogenetic tree. This was done iteratively, with each iteration, or factor, maximizing the F statistic from regression. Shown taxa represent either a single factor or combination of factors (when, for example, multiple factors identified different sOTUs with the same taxonomic classification). Labels represent either the highest taxonomic resolution or the highest classification shared by all sOTUs of a given clade. T0 = experiment commencement, TI = lesion genesis, TF = time of death. (B-D) Balance contrast of early (before lesion genesis) samples compared to late (immediately prior to lesion genesis) samples. Samples were transformed using the Phylogenetic Isometric Log-Ratio (PhILR; Silverman et al. 2017) transform, which uses a phylogenetic tree (B) to convert an sOTU table into a new matrix of coordinates derived from the ILR of clades that descend from a common node. We used a sparse logistic regression with an l_1 penalty of λ=0.15 (Silverman et al. 2017) to analyze the ILR at each node, and included a select number of 'balances' with positive coefficients (C-D). (C) is the balance of *Nitrosopumilus* (colored blue in (B), comprises the thin sliver on the right side of the tree) relative to the rest of the dataset (also shown in blue in (B)). A positive shift indicates an increase in *Nitrosopumilus* relative to its denominator. (D) is the balance between a clade of Alpha/Gammaproteobacteria (large, red clade in (B)) and Deltaproteobacteria (Bdellovibrionales and Desulfobacterales; small, red clade in (B)). A negative shift indicates that the denominator, Deltaproteobacteria, is increasing relative to Alpha/Gammaproteobacteria. (E) and (F) were derived from a PhyloFactor object and show the ILR balance of Flavobacteriales (E) and Rhodobacterales (F) relative to all other sOTUs. Time 0 = experiment commencement. All subsequent times show the day the sample was taken. Organic amendment is given above boxplots.

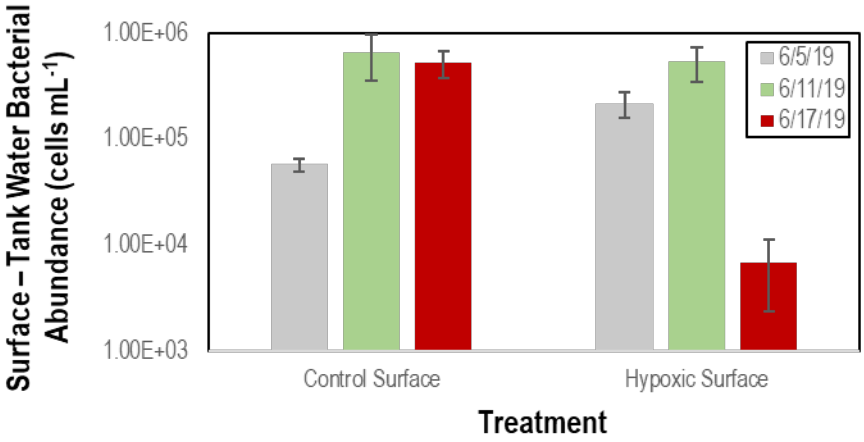

Fig. 2: Bacterial abundance in surface layer above *Asterias forbesi* during hypoxic and control treatments (n = 12 each). The abundance was corrected for aquarium water bacterial abundance and measured by SYBR Gold epilfluorescence microscopy.

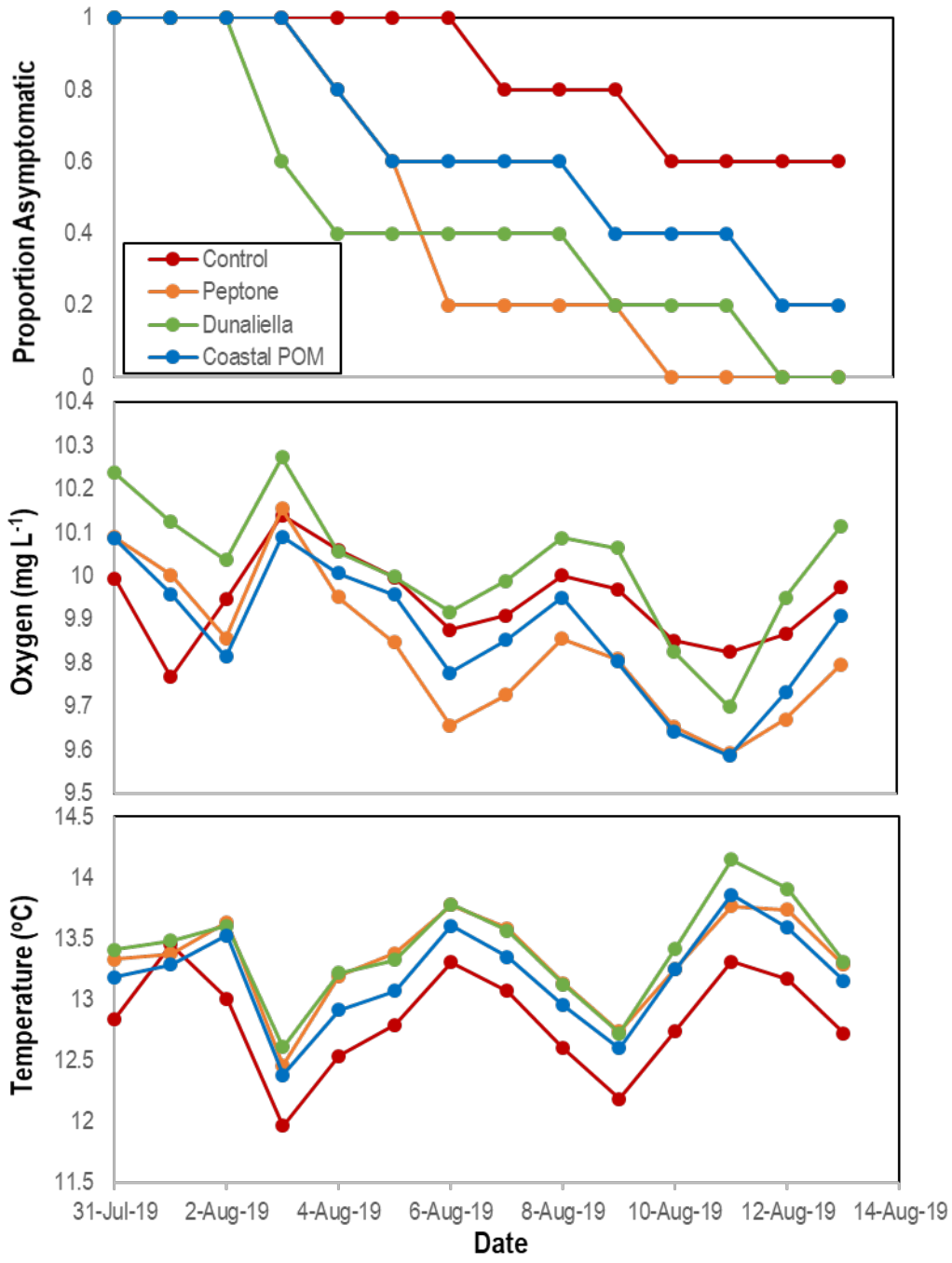

Fig 3: Proportion of asymptomatic *P. ochraceus* (n = 5 each treatment) incubated in flow-through conditions at the Bodega Marine Lab in response to organic matter enrichments (Peptone, *Dunaliella tertiolecta* culture POM, and coastal POM collected from the inflow at the Bodega Marine Laboratory in August 2019. Dissolved O_2 and temperature were measured in flow-through sea tables bearing each OM treatment.

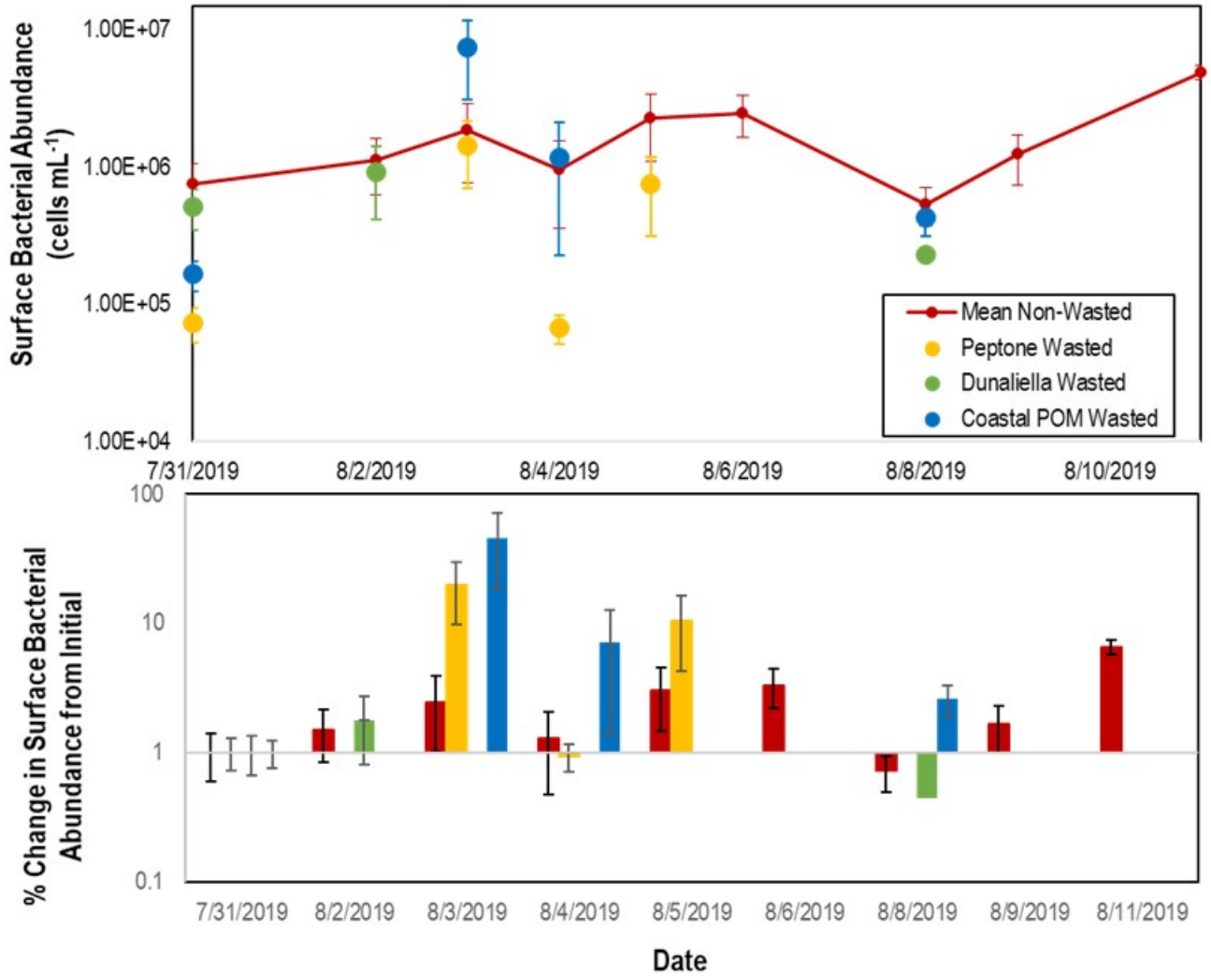

Fig 4: Abundance of bacteria in proximity to *P. ochraceus* surfaces (top) and percentage change from initial (below) during first 10 days of experiment in response to organic matter enrichment (n = 5 for each treatment) as assessed by SYBR Gold staining and epifluorescence microscopy. Non-wasted stars, regardless of treatment, are indicated in red, while the mean of stars that wasted in Peptone, *Dunaliella tertiolecta* POM, and Coastal POM are indicated separately.

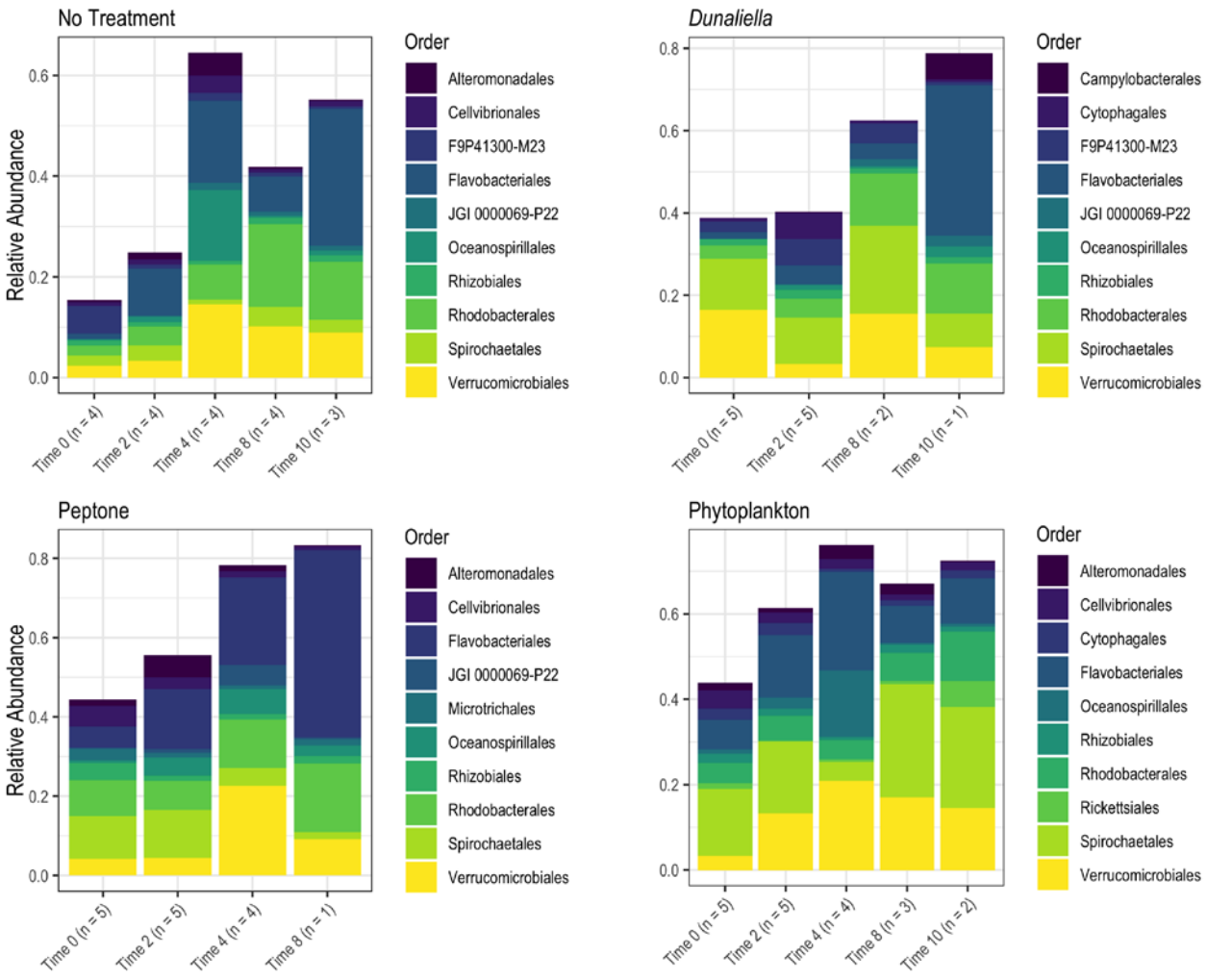

Fig 5: Relative abundance of bacterial orders derived from *P. ochraceus* epidermal swabs. Specimens were enriched with the indicated organic material and sampled until lesion genesis. Time 0 represents initial sampling and each subsequent time indicates the respective day. n values reflect the number of healthy specimens at each given timepoint.

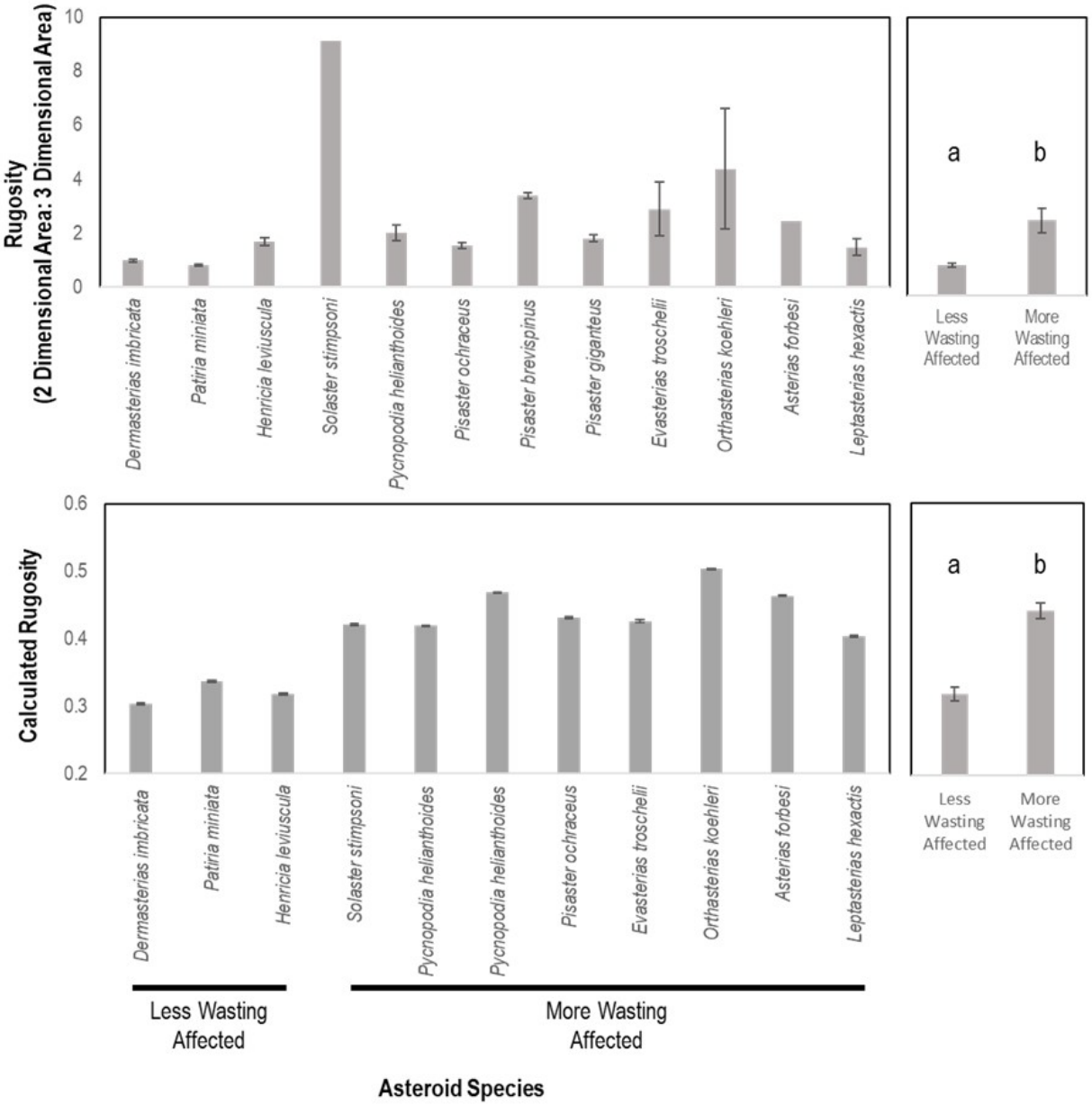

Fig. 6: Rugosity of similarly-sized animals between wasting-affected and less wasting affected species as determined by whole animal computed tomography (top) and of an asteroid ray by micro-computed tomography (bottom). a, b denote significant difference at $p < 0.001$.

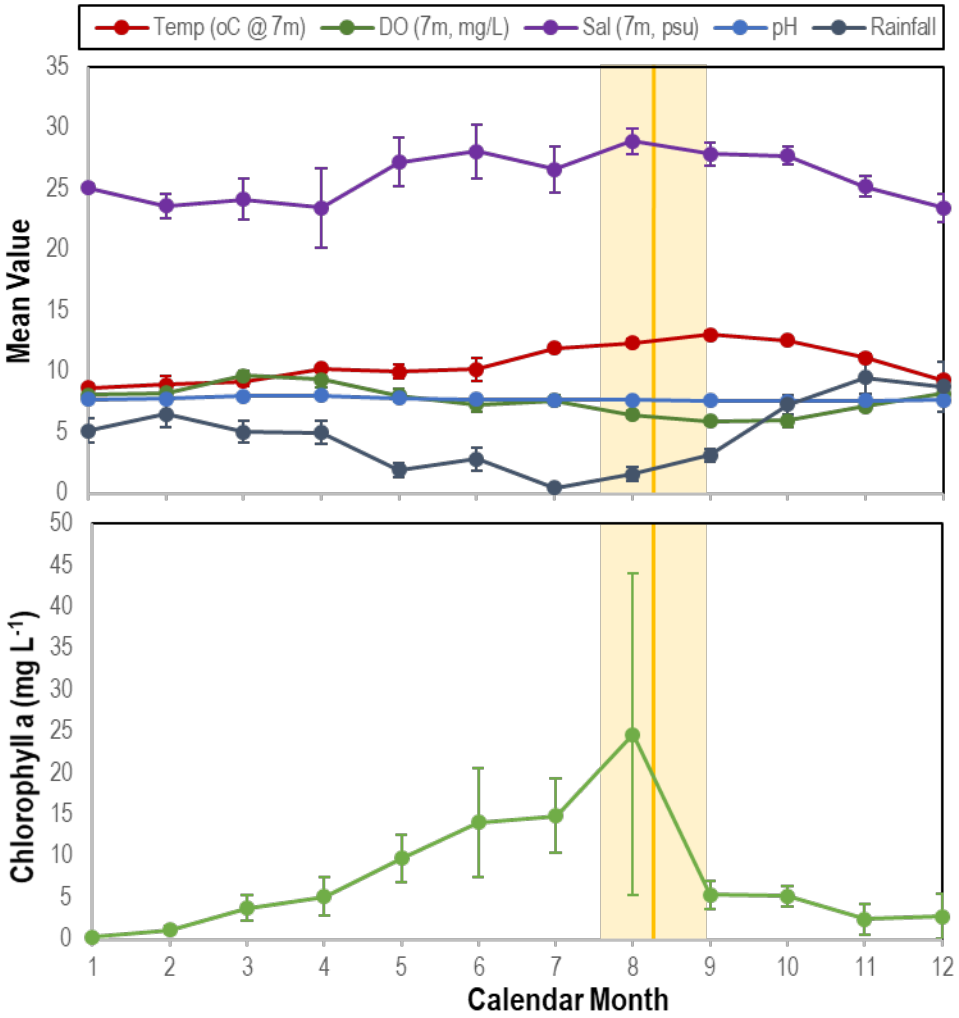

Fig 7: Correspondence between mean time of wasting mass mortality (indicated by solid orange line (SE range indicated by lighter orange bar) compared with physico-chemical parameters (top) and chlorophyll a concentration (bottom) at Penn Cove, Whidbey Island. Temp = temperature; DO = dissolved oxygen; Sal = salinity.

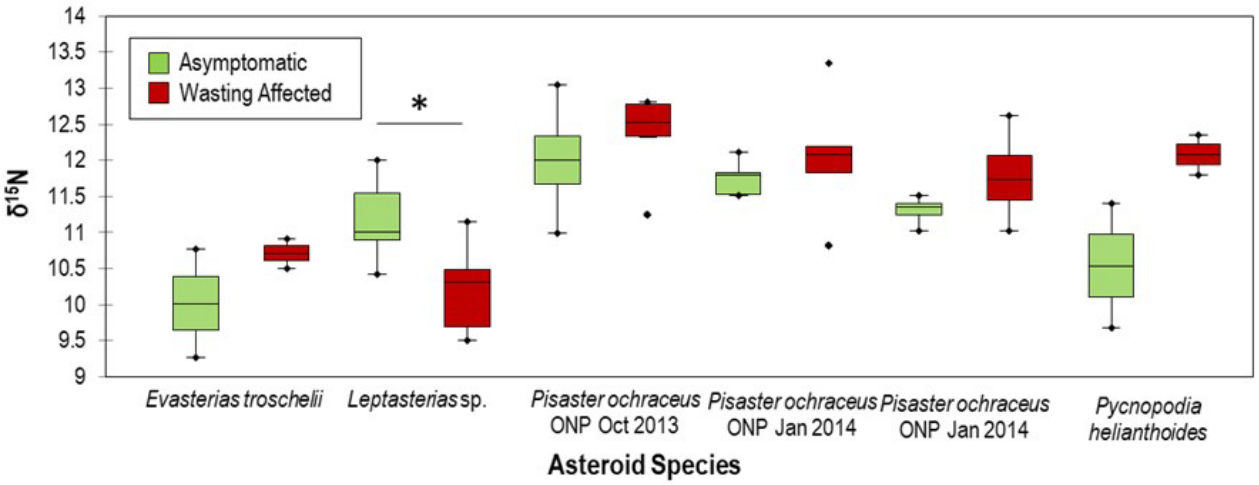

Fig. 8: Comparison of asymptomatic and wasting $\delta^{15}N$ values between species. ONP = Starfish point, Olympic national park and SC = Davenport, Santa Cruz, CA.